Accepted Manuscript

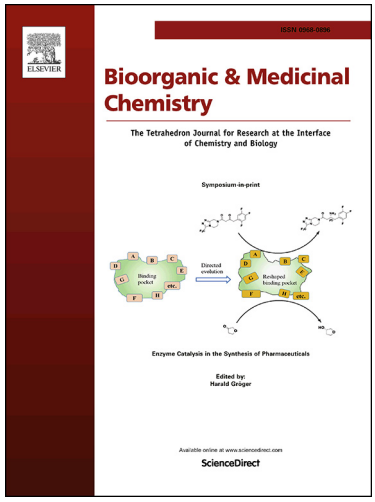

Leucine Ureido Derivatives as Aminopeptidase N Inhibitors Using Click Chemistry. Part II

Jiangying Cao, Jie Zang, Xiujie Kong, Chunlong Zhao, Ting Chen, Yingying Ran, Hang Dong, Wenfang Xu, Yingjie Zhang

PII: S0968-0896(18)32168-0
DOI: https://doi.org/10.1016/j.bmc.2019.01.041
Reference: BMC 14733

To appear in: *Bioorganic & Medicinal Chemistry*

Received Date: 27 December 2018
Revised Date: 27 January 2019
Accepted Date: 30 January 2019

Please cite this article as: Cao, J., Zang, J., Kong, X., Zhao, C., Chen, T., Ran, Y., Dong, H., Xu, W., Zhang, Y., Leucine Ureido Derivatives as Aminopeptidase N Inhibitors Using Click Chemistry. Part II, *Bioorganic & Medicinal Chemistry* (2019), doi: https://doi.org/10.1016/j.bmc.2019.01.041

Leucine Ureido Derivatives as Aminopeptidase N Inhibitors Using Click Chemistry. Part II

Jiangying Cao[a], Jie Zang[a], Xiujie Kong[a], Chunlong Zhao[a], Ting Chen[a], Yingying Ran[a], Hang Dong[a], Wenfang Xu[a], Yingjie Zhang[a,*]

[a]*Department of Medicinal Chemistry, School of Pharmaceutical Sciences, Shandong University, Jinan 250012, P. R. China*

*Corresponding Author. Tel/Fax: +86 531 88382009

E-mail address: zhangyingjie@sdu.edu.cn (Y. Zhang).

Abstract

Aminopeptidase N (APN) has been proved to be deeply associated with cancer angiogenesis, metastasis and invasion. Therefore, APN gains increasing attention as a promising anti-tumor target. In the current study, we report the design, synthesis, biological evaluation and structure-activity relationship of one new series of leucine ureido derivatives containing the 1,2,3-triazole moiety. Among them, compound **31f** was identified as the best APN inhibitor with IC_{50} value being two orders of magnitude lower than that of the positive control bestatin. Compound **31f** possessed selective cytotoxicity to several tumor cell lines over the normal cell line human umbilical vein endothelial cells (HUVECs). Notably, when combined with 5-fluorouracil (5-Fu), **31f** exhibited synergistic anti-proliferation effect against several tumor cell lines. At the same concentration, **31f** exhibited much better anti-angiogenesis activities than bestatin in the HUVECs capillary tube formation assay and the rat thoracic aorta rings test. In the *in vitro* anti-invasion assay, **31f** also exhibited superior potency over bestatin. Moreover, considerable *in vivo* antitumor potencies of **31f** alone or in combination with 5-Fu were observed without significant toxic signs in a mouse heptoma H22 tumor transplant model.

Key words: aminopeptidase N; CD13; anti-angiogenesis; anti-metastasis; triazole.

1. Introduction

Aminopeptidase N (APN; CD13; EC 3.4.11.2) is a widely expressed Zn^{2+} dependent membrane-bound exopeptidase belonging to the M1 family of the MA clan of peptidase.[1,2] The full length 967 amino acids of aminopeptidase N can be divided into three parts: a short cytoplasmic domain, a single transmembrane part and a large extracellular domain containing the active site.[3] It is known to preferentially release basic or neutral amino acids from the *N*-terminus of the biologically active peptides.[4] APN is a moonlighting protein possessing the enzymatic as well as other functions, such as antigen presentation and the receptor for some viruses.[5] Enhanced APN expression has been observed on diverse malignancies, such as melanoma[6], renal[7], colon[8], prostate[9] and gastric[10] carcinomas. The expression of APN is related to the regulation of signal peptides and is associated with the tumor migration, invasion, metastasis and angiogenesis.[11-17] It was revealed that APN could degrade the extracellular matrix (ECM) to promote malignant cells invasion and metastasis.[15,16] Recently, it was reported that the APN expressed by both cancer cells and nonmalignant stromal cells within the tumor environment could cooperatively promote the angiogenesis.[17] Moreover, APN is a functional marker of semi-dormant liver cancer cells that are responsible for chemotherapy resistance and cancer relapse.[18]

Because of the significant role of APN in cancer, the rational design of potent APN inhibitors as antitumor agents is of considerable interest. To date, several classes of APN inhibitors (APNIs) have been reported (Figure 1), including AHPA ((2*S*, 3*R*)-3-amino-2-hydroxy-4-phenylbutanoic acid) derivative **1** (bestatin), hydroxamic acid derivative **2** (tosedostat), mercaptan derivative **3** (PC18), amino-benzosuberone derivative **4**, boronic acid derivative **5**, aminophosphinic derivative **6** (PL253), L-isoserine derivative **7**, flavone derivative **8**, dicarbonyl derivative **9**, L-arginine

derivative **10**, chloramphenicol amine derivative **11** and 3-phenylpropane-1,2-diamine derivative **12**.[19-21]

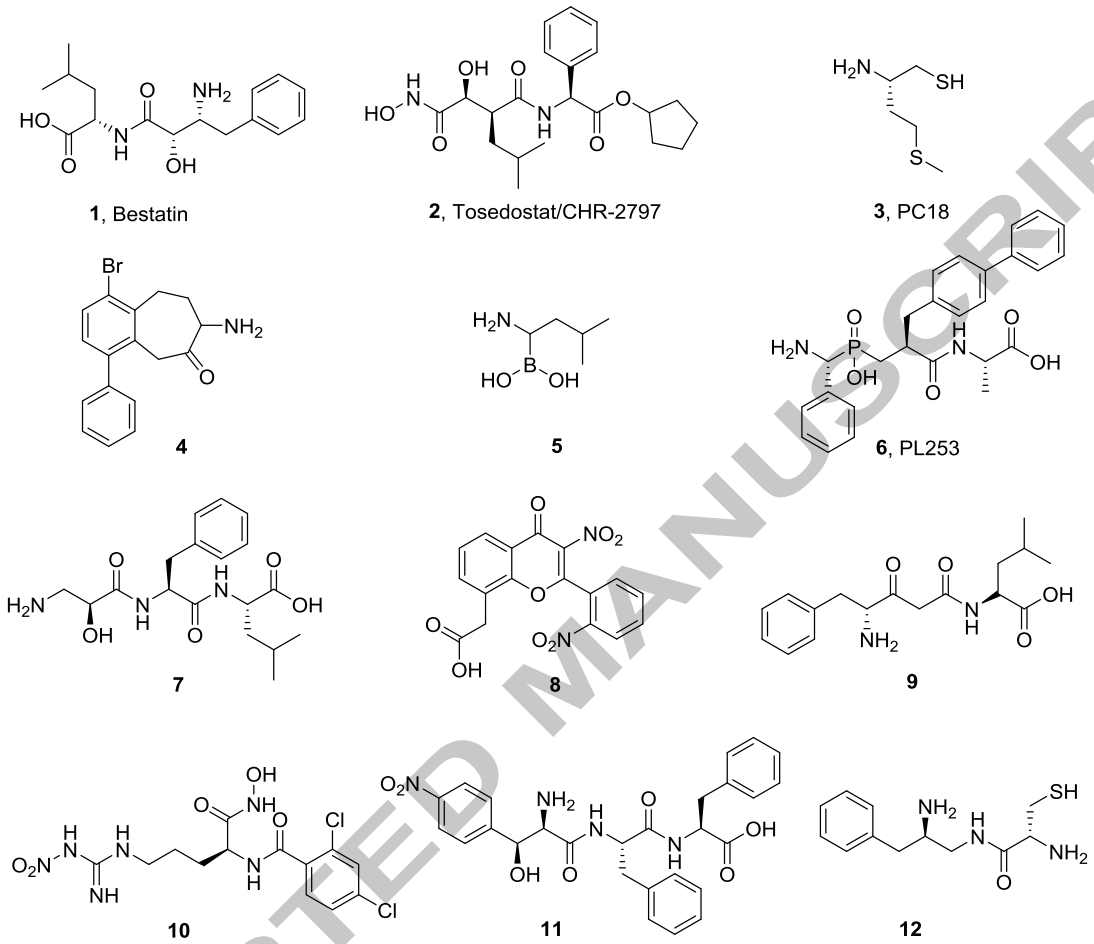

Figure 1. Structures of representative APNIs.

So far, bestatin, with an AHPA skeleton, has been approved as the adjuvant for the treatment of adult acute non-lymphocytic leukaemia. Recently, bestatin was found to have broad spectrum of biological activities, such as anti-angiogenic, anti-metastatic, and immunomodulatory effects.[22-23] Our group has been pursuing the development of APNIs as anticancer agents for a long time.[24-30] In our previous work, the leucine ureido derivatives with the 1,2,3-triazole moiety (**13**, Figure 2) exhibited excellent APN inhibitory potency and promising *in vitro* and *in vivo* anti-angiogenesis and anti-metastasis effect.[31] Herein, to extend the structure-activity relationships (SARs) of these leucine ureido derivatives, a new series of analogues **14** was designed and synthesized.

Compared with **13**, the terminal substituted phenyl group of **14** (Figure 2) was directly attached to the triazole moiety to investigate the effect of conformational restriction on APN inhibition. Besides, one carboxylic acid derivative and two isoleucine and methionine derivatives (Figure 2) were also synthesized to respectively investigate the effects of the zinc binding group (ZBG) and the side chain on APN inhibition.

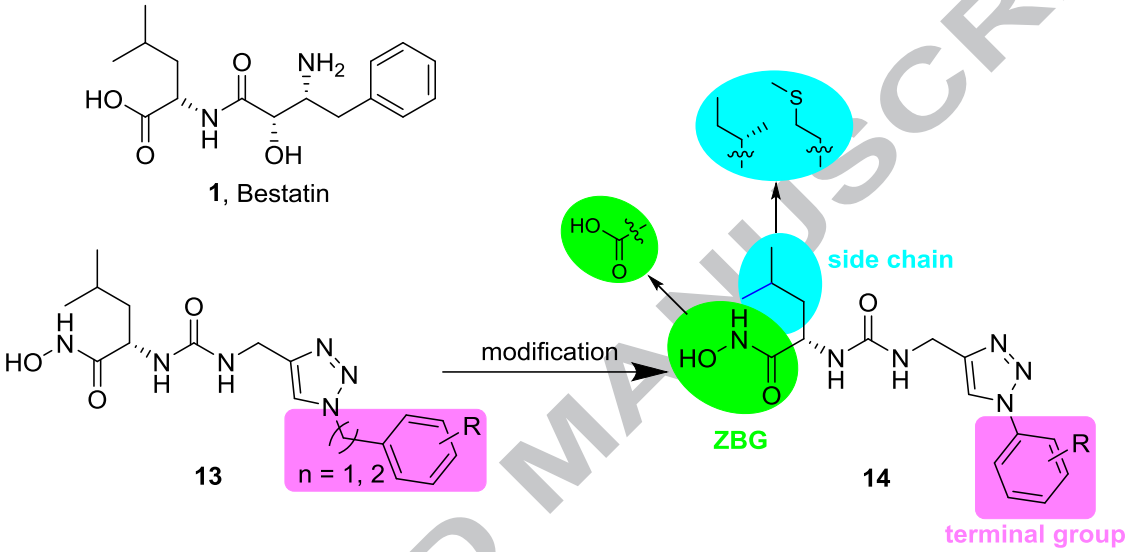

Figure 2. The structure of bestatin and the design strategy of novel APNIs.

2. Chemistry

The synthetic routes of target compounds are shown in Schemes 1-4. As shown in Scheme 1, compounds **15a-15c** reacted with triphosgene to generate isocyanates, which were then immediately reacted with propargylamine to yield the ureido derivatives **16a-16c**. The ureido derivatives **16a-16c** reacted with sodium hydroxide or NH_2OK to generate the key intermediates **17** or **18a-18c**, respectively.

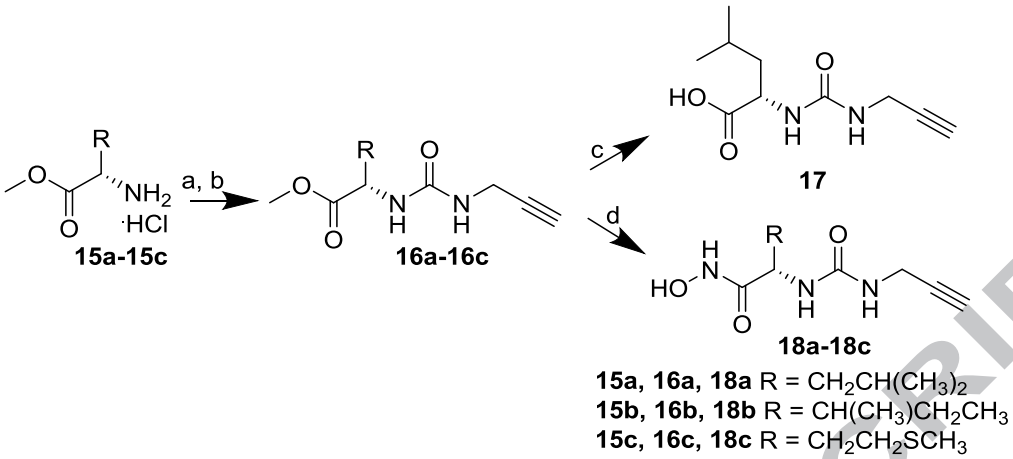

Scheme 1. Reagents and conditions: (a) triphosgene, $NaHCO_3$, DCM/H_2O, 0 °C, 1.5 h; (b) propargylamine, TEA, DCM, 25 °C, 12 h; (c) **16a** for **17,** NaOH, H_2O, MeOH, 25 °C, 0.5 h; (d) NH_2OK, MeOH, 25 °C, 0.5 h.

As shown in Scheme 2, activation of the amino groups of the aromatic amines **19a-19z** and **19aa** with sodium nitrite in 10% hydrochloric acid and then reaction with sodium azide led to the azide derivatives **20a-20z** and **20aa**. Compound **20a** was coupled with **17**, **18b** or **18c** *via* click chemistry to give target compounds **21**, **23** or **24**, respectively. The target compounds **22a-22z** and **22aa** were respectively generated by coupling **18a** with **20a-20z** and **20aa** *via* click chemistry.

Scheme 3 presented the synthesis of the key intermediate **28**. Compound **27** was prepared using compound **25** as the starting material according to the method reported before.[31] Activation of the amino group of compound **27** with sodium nitrite in 10% hydrochloric acid and then reaction with sodium azide led to the key intermediate **28**. Compound **28** reacted with **29a-29i** to generate compounds **30a-30i**, which were then coupled with **18a** to give the target compounds **31a-31i** (Scheme 4).

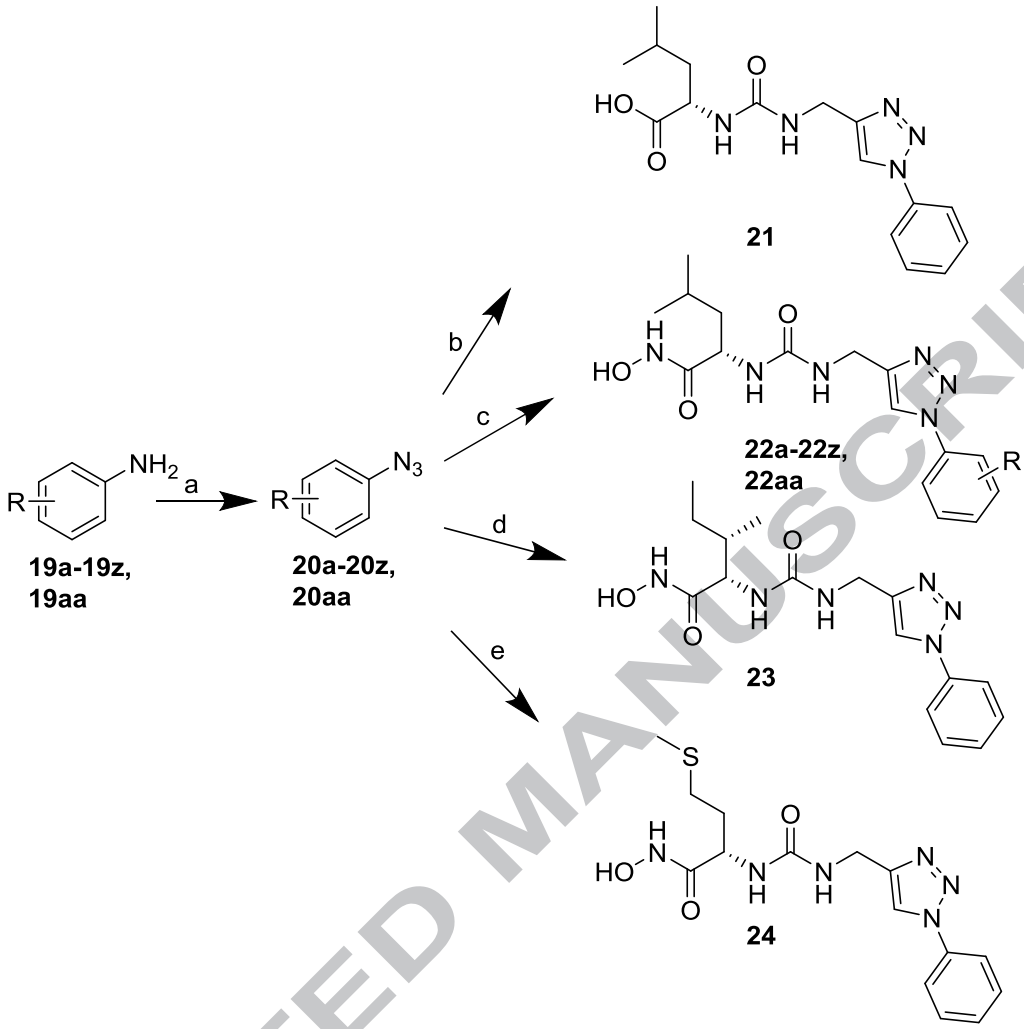

19a, 20a, 22a R_1 = H,
19b, 20b, 22b R_1 = 2-Cl,
19c, 20c, 22c R_1 = 3-Cl,
19d, 20d, 22d R_1 = 4-Cl,
19e, 20e, 22e R_1 = 2-Br,
19f, 20f, 22f R_1 = 3-Br,
19g, 20g, 22g R_1 = 4-Br,
19h, 20h, 22h R_1 = 2-CH_3,
19i, 20i, 22i R_1 = 3-CH_3,
19j, 20j, 22j R_1 = 4-CH_3,
19k, 20k, 22k R_1 = 2-OH,
19l, 20l, 22l R_1 = 3-OH,
19m, 20m, 22m R_1 = 4-OH,
19n, 20n, 22n R_1 = 2-OCH_3,
19o, 20o, 22o R_1 = 3-OCH_3,
19p, 20p, 22p R_1 = 4-OCH_3,
19q, 20q, 22q R_1 = 2-$COOCH_3$,
19r, 20r, 22r R_1 = 2-OCH_2CH_3,
19s, 20s, 22s R_1 = 2,6-diCH_3,
19t, 20t, 22t R_1 = 2,6-diCl,
19u, 20u, 22u R_1 = 2,5-diCl,
19v, 20v, 22v R_1 = 2,6-diOCH_3,
19w, 20w, 22w R_1 = 2,6-diOCH_2CH_3,
19x, 20x, 22x R_1 = 3,5-diCl,
19y, 20y, 22y R_1 = 3,4-diCH_3,
19z, 20z, 22z R_1 = 3-Cl-4-CH_3,
19aa, 20aa, 22aa R_1 = 3,5-diCH_3.

Scheme 2. Reagents and conditions: (a) i: 10% HCl, $NaNO_2$, 0 °C, 0.5 h, ii: NaN_3, 0 °C, 0.5 h; (b) **17** for **20a**, $CuSO_4{\cdot}5H_2O$, sodium ascorbate, DMSO/H_2O (4:1), 25 °C, 2 h; (c) **18a** for **20a-20z** or **20aa**, $CuSO_4{\cdot}5H_2O$, sodium ascorbate, DMSO/H_2O (4:1), 25 °C, 2 h; (d) **18b** for **20a,** $CuSO_4{\cdot}5H_2O$, sodium ascorbate, DMSO/H_2O (4:1), 25 °C, 2 h; (e) **18c** for **20a,** $CuSO_4{\cdot}5H_2O$, sodium ascorbate, DMSO/H_2O (4:1), 25 °C, 2 h.

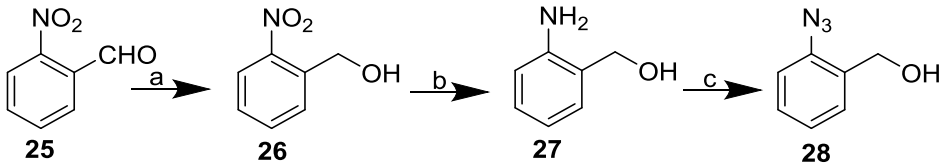

Scheme 3. Reagents and conditions: (a) $NaBH_4$, MeOH, 0 °C, 1 h; (b) $Na_2S{\cdot}9H_2O$, H_2O, 100 °C, 3 h; (c) i: 10% HCl, $NaNO_2$, 0 °C, 0.5 h, ii: NaN_3, 0 °C, 0.5 h.

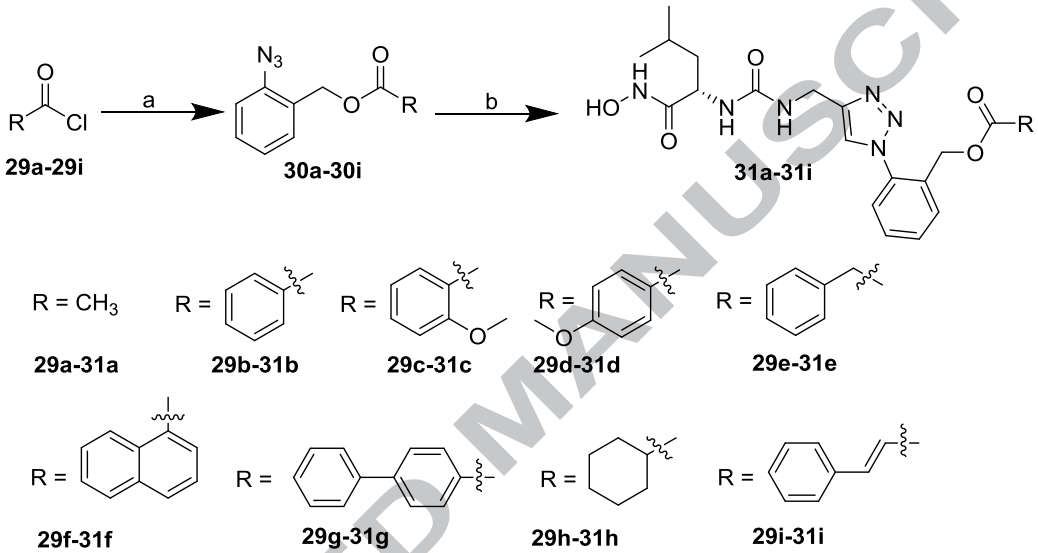

Scheme 4. Reagents and conditions: (a) **28**, Et_3N, THF, 50 °C, 3 h; (b) **18a** for **30a-30i,** $CuSO_4{\cdot}5H_2O$, sodium ascorbate, DMSO/H_2O (4:1), 25 °C, 2 h.

3. Results and discussion

3.1. Enzyme inhibitory activities of the target compounds against porcine APN

All the target compounds synthesized were firstly evaluated for their inhibitory activities against porcine APN (Microsomal, Biocol) with bestatin as the positive control. The results in Table 1 showed that compound **22a** was over 18-fold more potent than bestatin. It was also revealed that **22a** exhibited 4-fold and 7-fold improved APN inhibitory activities relative to **13a** and **13b**, respectively, indicating the beneficial effect of conformational restriction on APN inhibition. The carboxylic acid derivative **21** exhibited much less APN inhibitory activity than its corresponding hydroxamic acid derivative **22a**, suggesting the significant role of hydroxamic acid as the strong ZBG in

APN inhibition. Moreover, comparing **22a** with **23** and **24**, it was easy to find that the replacement of leucine residue with isoleucine or methionine residue was detrimental to APN inhibition. Therefore, **22a** was selected as the lead compound for further structural optimization and modification. Introduction of various substituents on the terminal phenyl group of **22a** led to mono-substituted analogs **22b-22r**, and dual-substituted analogs **22s-22z** and **22aa**. For compounds with single halogen (**22b-22g**), single methyl (**22h-22j**) or single methoxyl (**22n-22p**) substituents, the *ortho*-substituted compounds (**22b**, **22e**, **22h, 22n**) exhibited better activities than their *meta*- (**22c**, **22f**, **22i, 22o**) or *para*-substituted (**22d**, **22g**, **22j, 22p**) analogs. However, this trend was not observed in compounds with single hydroxyl (**22k-22m**) substituents. Generally, mono-substituents on the terminal phenyl group of **22a** were tolerated, leading to several compounds (**22b**, **22e**, **22l**, **22m**, **22n, 22q**, **22r**) with improved activities relative to **22a**, however, most of the dual-substituents were detrimental, especially compared with their corresponding mono-substituents. Note that the most potent mono-substituted analogs (**22q, 22r**) and the most potent dual-substituted analog (**22w**) all possessed larger substituents at the *ortho*-position. Therefore, analogs with extra-large *ortho*-substituents (**31a-31i**) were synthesized and evaluated. Satisfyingly, all these compounds except **31g** exhibited better APN inhibitory activities than **22a**. The most potent compound **31f** (IC_{50} = 0.032 ± 0.003 μM) was over 15-fold more potent than **22a** (IC_{50} = 0.51 ± 0.02 μM) and over 293-fold more potent than the positive control bestatin (IC_{50} = 9.4 ± 0.5 μM).

Table 1. The structures and IC_{50} values of target compounds against APN from porcine kidney.

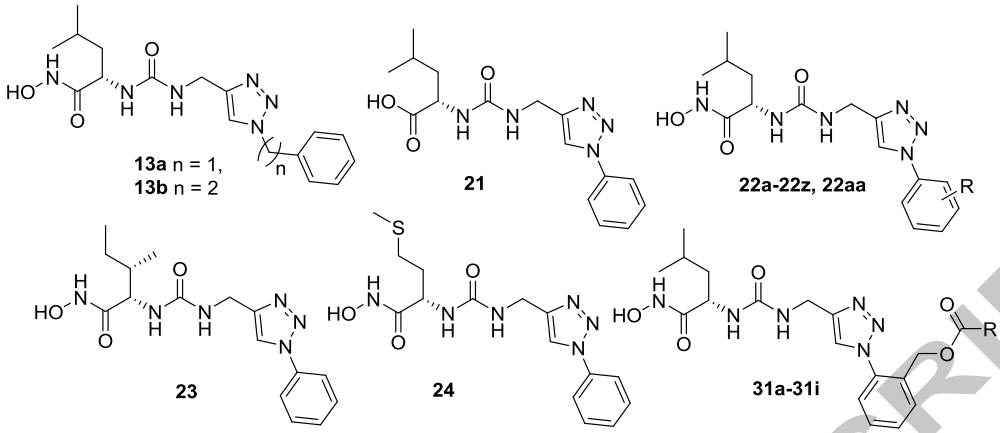

Compd	R	IC_{50} (μM)[a]	Compd	R	IC_{50} (μM)[a]
13a	--	2.1 ± 0.2[b]	**22s**	2,6-diCH_3	1.5 ± 0.3
13b	--	3.6 ± 0.3[b]	**22t**	2,6-diCl	0.36 ± 0.03
21	--	98.9 ± 8.6	**22u**	2,5-diCl	1.1 ± 0.2
22a	H	0.51 ± 0.02	**22v**	2,6-diOCH_3	0.58 ± 0.05
22b	2-Cl	0.28 ± 0.02	**22w**	2,6-diOCH_2CH_3	0.30 ± 0.01
22c	3-Cl	1.9 ± 0.2	**22x**	3,5-diCl	3.6 ± 0.2
22d	4-Cl	1.2 ± 0.3	**22y**	3,4-diCH_3	1.8 ± 0.1
22e	2-Br	0.40 ± 0.01	**22z**	3-Cl-4-CH_3	2.7 ± 0.2
22f	3-Br	1.9 ± 0.1	**22aa**	3,5-diCH_3	1.7 ± 0.2
22g	4-Br	1.7 ± 0.2	**23**	--	19.3 ± 1.4
22h	2-CH_3	0.60 ± 0.05	**24**	--	4.1 ± 0.4
22i	3-CH_3	4.8 ± 0.4	**31a**	CH_3	0.42 ± 0.04
22j	4-CH_3	2.5 ± 0.3	**31b**		0.12 ± 0.01
22k	2-OH	0.52 ± 0.01	**31c**		0.16 ± 0.02
22l	3-OH	0.34 ± 0.03	**31d**	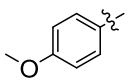	0.27 ± 0.02
22m	4-OH	0.30 ± 0.01	**31e**	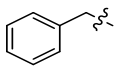	0.26 ± 0.01

22n	2-OCH_3	0.47 ± 0.01	**31f**	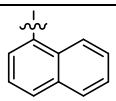	0.032 ± 0.003
22o	3-OCH_3	0.54 ± 0.05	**31g**	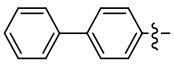	1.2 ± 0.2
22p	4-OCH_3	0.50 ± 0.03	**31h**		0.33 ± 0.02
22q	2-$COOCH_3$	0.25 ± 0.01	**31i**	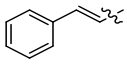	0.085 ± 0.004
22r	2-OCH_2CH_3	0.26 ± 0.03	Bestatin	--	9.4 ± 0.5

[a]Assays were performed in triplicate; data are shown as mean ± SD. [b]Reported in reference 31.

3.2. Enzyme inhibitory activities of the selected compounds against human APN on the surface of ES-2 and PLC/PRF/5 cells

Furthermore, we evaluated the inhibitory potency of selected compounds **31b**, **31c**, **31d**, **31f** and **31i** against human APN located on the surface of the ES-2 and PLC/PRF/5 cells. Both cell lines have been proved to have relatively higher APN expression on the cell membrane. The results are listed in Table 2. All the selected compounds exhibited much better activities than the positive control bestatin (IC_{50} = 35.5 ± 2.3 μM for ES-2 cell surface APN, IC_{50} = 54.7 ± 3.5 μM for PLC/PRF/5 cell surface APN), and the human APN inhibitory order is **31f** > **31i** > **31b** > **31c** > **31d**, which was consistent with the results of inhibition against porcine APN. The most potent compound **31f** possessed IC_{50} values of 0.39 ± 0.01 μM and 0.81 ± 0.04 μM against APN on the surface of ES-2 and PLC/PRF/5 cells, respectively.

Table 2. The IC_{50} values of selected compounds against APN on ES-2 and PLC/PRF/5 cell surfaces.

Compd	IC_{50} (μM)[a]		Compd	IC_{50} (μM)[a]	
	ES-2	PLC/PRF/5		ES-2	PLC/PRF/5
31b	0.65 ± 0.07	1.4 ± 0.3	**31f**	0.39 ± 0.01	0.81 ± 0.04
31c	0.99 ± 0.08	2.3 ± 0.2	**31i**	0.62 ± 0.03	1.2 ± 0.1
31d	1.1 ± 0.1	3.3 ± 0.3	Bestatin	35.5 ± 2.3	54.7 ± 3.5

[a]Assays were performed in triplicate; data are shown as mean ± SD.

3.3. In vitro anti-proliferative activities of the selected compounds

Compound **31f** with the most potent porcine and human APN inhibitory activity was further evaluated in the anti-proliferation assay against six tumor cell lines (PLC, K562, A549, ES-2, PC-3 and H7402) and one normal cell line (the human umbilical vein endothelial cell, HUVEC). The results in Table 3 showed that **31f** exhibited much superior anti-proliferative potencies than bestatin against all the tested tumor cell lines. Importantly, the IC_{50} value of **31f** against HUVEC was > 2000 μM, demonstrating its selective cytotoxicity against tumor cells over normal cells.

Recently, bestatin was reported to show synergistic anti-tumor effects in combination with chemotherapy drugs, such as 5-fluorouracil (5-Fu), cisplatin (CDDP), and doxorubicin (DXR).[32] Encouraged by this, we also evaluated the anti-proliferative effects of **31f** plus 5-Fu. The combination index (CI) calculated based on the Chou−Talalay method was used to evaluate the combined effects of **31f** and 5-Fu.[33] As shown in Table 3, the CI values for all the tested tumor cell lines were less than 1, indicating the synergistic effects of the combination of **31f** and 5-Fu in inhibiting the proliferation of tumor cells.

Table 3. *In vitro* antiproliferative activities of selected compounds.

Compd	IC_{50} (μM)[a]						
	PLC	K562	A549	ES-2	PC-3	H7402	HUVEC
31f	64.3 ± 3.1	40.6 ± 0.2	57.5 ± 5.5	61.2 ± 3.5	63.2 ± 1.5	52.6 ± 4.3	> 2000
5-Fu	116.8 ± 5.4	20.7 ± 5.7	38.7 ± 8.4	37.9 ± 4.9	49.1 ± 5.8	76.3 ± 6.8	ND[b]
Bestatin	> 500	> 500	> 500	> 500	> 500	> 500	> 2000
31f + 5-Fu[c]	17.1 ± 1.0 (CI = 0.4)[d]	6.9 ± 0.4 (CI = 0.5)	16.6 ± 1.7 (CI = 0.7)	10.3 ± 1.0 (CI = 0.4)	17.6 ± 2.2 (CI = 0.6)	15.2 ± 0.4 (CI = 0.5)	ND[b]

[a] Assays were performed in triplicate; data are shown as mean ± SD. [b] Not determined. [c] Combined at the mole ratio of 1:1. [d] CI > 1 indicates antagonism, CI = 1 indicates an additive effect, and CI < 1 indicates synergism.

3.4. In vitro and ex vivo anti-angiogenesis assays

To compare the anti-angiogenic effects of compound **31f** and bestatin, the *in vitro* HUVEC tubular structure formation assay was performed. As shown in Figure 3A, both bestatin and **31f** could obviously decrease the HUVEC tubular structure formation at their noncytotoxic concentrations (the IC_{50} values of bestatin and **31f** against HUVEC were over 2000 μM, as shown in Table 3). Moreover, compound **31f** inhibited the HUVEC tube formation in a dose-dependent manner, the inhibiting rate of compound **31f** at 10 μM was comparable to that of bestatin at 100 μM (Figure 3B), revealing the superior anti-angiogenic activity of **31f**. When the concentration of **31f** was increased to 100 μM, no obvious tubular structures were observed.

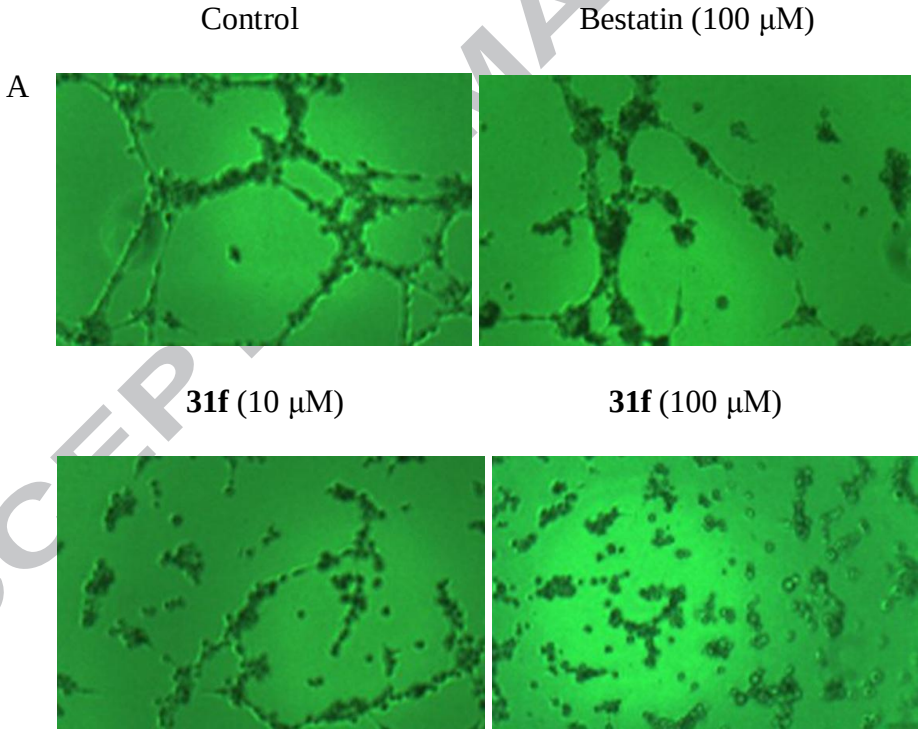

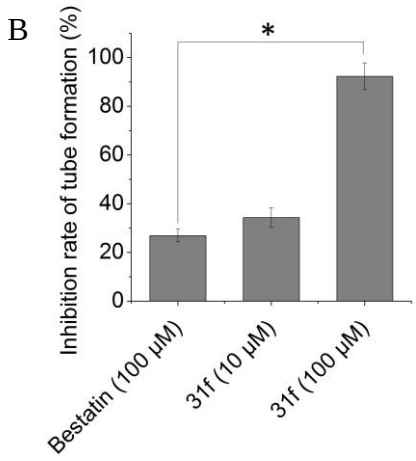

Figure 3. (A) Representative images of the capillary-like tubular network of HUVECs treated with DMSO (0.5%) or compounds. (B) The inhibition rates of tested compounds on the HUVEC tubular structure formation. Data are expressed as the mean ± standard deviation from triplicate experiments. * $P < 0.05$.

The *ex vivo* rat thoracic aorta ring assay was used to further evaluate the anti-angiogenic activity of compound **31f**. As shown in Figure 4, **31f** exhibited the capacities of inhibiting the micro-vessels growth in a dose-dependent manner. At the concentration of 100 μM, **31f** almost completely inhibited the micro-vessels growth, much more potent than bestatin.

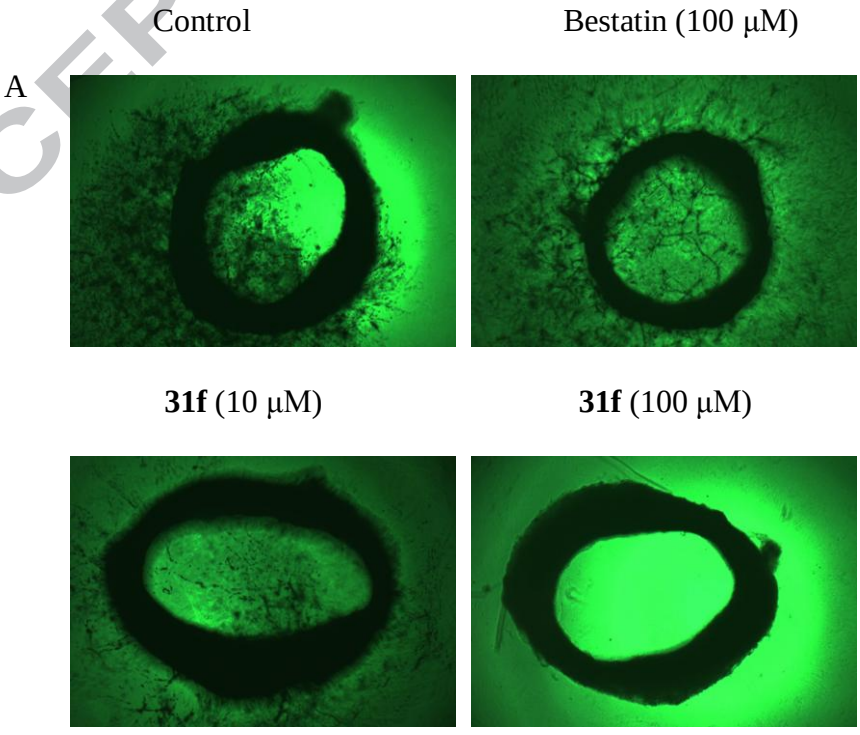

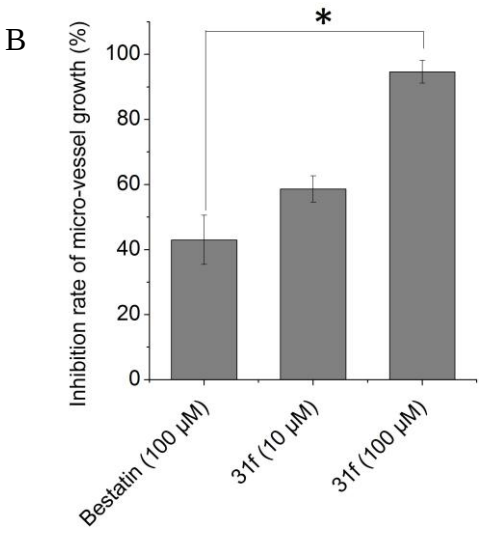

Figure 4. (A) Representative images of the rat thoracic aorta rings treated with DMSO (0.5%) or compounds. (B) The inhibition rates of tested compounds on the micro-vessels growth. Data are expressed as the mean ± standard deviation from triplicate experiments. * $P < 0.05$.

3.5. In vitro anti-invasion assay

Tumor cell invasion plays an important role in the progress of cancer metastasis. In this research, an anti-invasion assay was performed on transwell chambers coated with Matrigel. As shown in Figure 5, ES-2 cell could freely invade and pass through Matrigel in the negative control group, while this progress was dramatically impeded by **31f** and bestatin at their noncytotoxic concentrations (the IC_{50} values of **31f** and bestatin against ES-2 cells were 61.2 ± 3.5 μM and ＞ 500 μM, respectively, as shown in Table 3). Actually, after 8 h treatment (the time needed for the anti-invasion assay) with 10 μM of **31f**, the growth inhibition rate of ES-2 cells was around 1.4%, which confirmed that the anti-invasion effect of **31f** was not due to its cytotoxicity. Notably, 10 μM of **31f** exhibited comparable, if not better anti-invasion activity than 100 μM of bestatin.

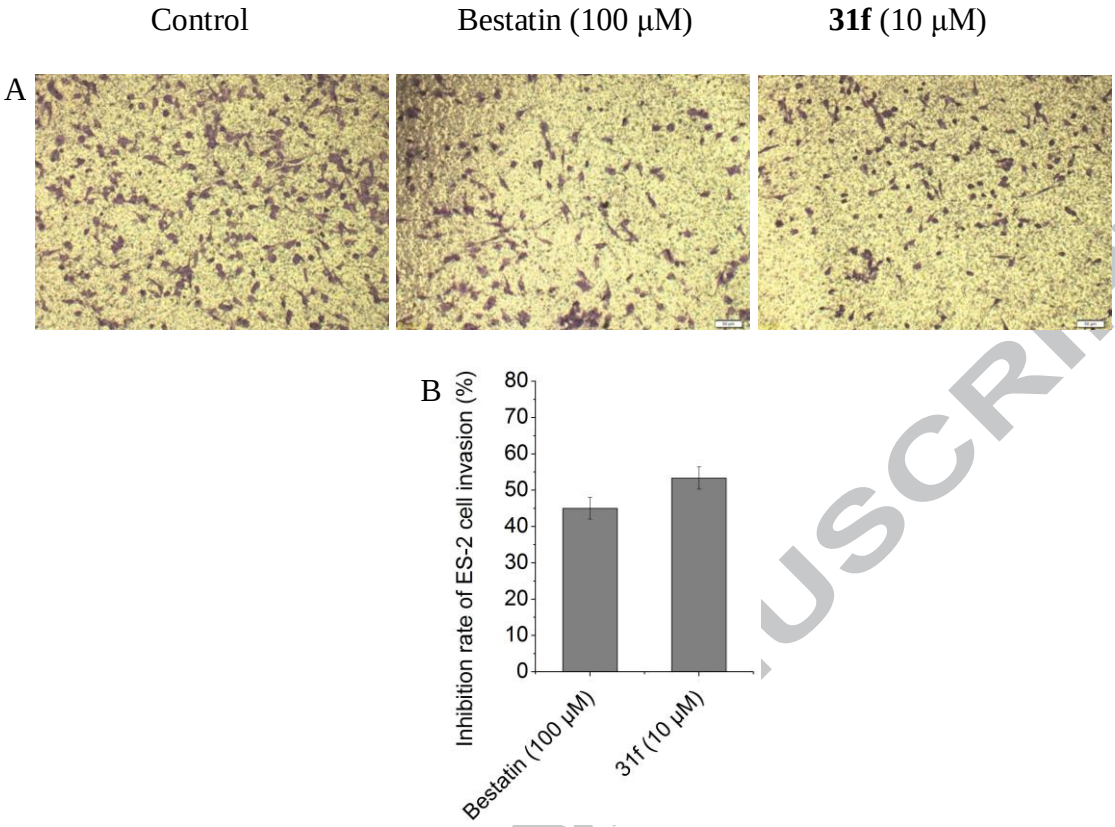

Figure 5. (A) Representative images of ES-2 cell invasion treated with DMSO (0.5%) or compounds. (B) The inhibition rates of tested compounds on the ES-2 cell invasion. Data are expressed as the mean ± standard deviation from triplicate experiments.

3.6. In vivo antitumor evaluation

Encouraged by its promising antiproliferation, anti-angiogenesis and anti-invasion potencies, **31f** was progressed to the *in vivo* antitumor evaluation in a mouse heptoma H22 tumor transplant model. As shown in Figure 6A and 6B, intraperitoneal administration of **31f** alone or in combination with 5-Fu could effectively inhibit tumor growth. It was worth noting that **31f** (82 mg/kg, equivalent to 154 μmol/kg) plus 5-Fu (20 mg/kg, equivalent to 154 μmol/kg) exhibited more potent anti-tumor activity than **31f** (82 mg/kg, equivalent to 154 μmol/kg) alone or 5-Fu (20 mg/kg, equivalent to 154 μmol/kg) alone, which was in line with their synergistic antiproliferation activity shown in Table 3. What's more, at the same molar concentration, the *in vivo* anti-tumor potency of **31f** (82 mg/kg, equivalent to 154 μmol/kg) plus 5-Fu (20 mg/kg, equivalent

to 154 μmol/kg) was similar to that of bestatin (47 mg/kg, equivalent to 154 μmol/kg) plus 5-Fu (20 mg/kg, equivalent to 154 μmol/kg). During the experiment, the body weights of mice were monitored every two days. Interestingly, in contrast to the mice group treated with 5-Fu alone, no body weight loss was observed in mice groups treated with **31f** alone or in combination with 5-Fu (Figure 6C).

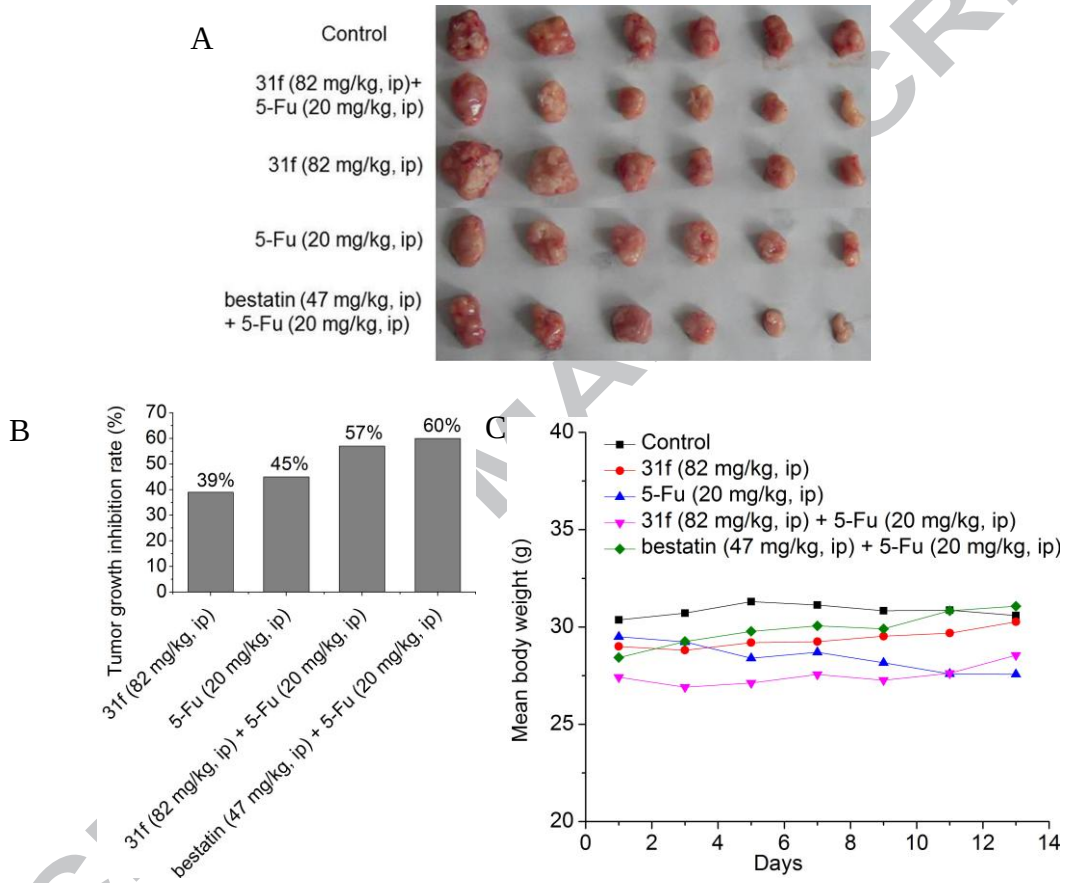

Figure 6. *In vivo* antitumor effects in a mouse heptoma H22 tumor transplant model. (A) The pictures of dissected tumor tissues. (B) Tumor growth inhibition rate. (C) Mean mice body weights monitored every two days.

4. Conclusion

In summary, extended SARs of previously reported leucine ureido-based APNI were conducted and led to abundant compounds with better APN inhibitory potency than the positive control bestatin. *In vitro* biological evaluation of the most potent compound **31f** revealed its potent anti-proliferation, anti-angiogenesis and anti-invasion activities. The

following *in vivo* antitumor evaluation showed that **31f** alone or in combination with 5-Fu could effectively inhibit tumor growth in a mouse heptoma H22 tumor transplant model. These results support the further research and development of **31f** as a promising antitumor lead compound.

5. Experimental section

5.1. Chemistry: General procedures

All the commercially available materials (Adamas-beta) were used without further purification otherwise noted. All reactions were monitored by thin-layer chromatography (TLC) on 0.25 mm silica gel plates (60 GF-254) and visualized by UV light, ferric chloride and iodine vapor. Column chromatography and recrystallization were used to purify the products. Melting points were determined on an electrothermal melting point apparatus without correction. ^{1}H-NMR and ^{13}C-NMR spectra were determined on a Brucker DRX spectrometer with TMS as an internal standard. Chemical shifts were described as δ in parts per million and J in Hertz. HRMS and ESI-MS were conducted by Shandong Analysis and Test Center.

*5.1.1. Preparation of compounds **16a-16c***

Compounds methyl (prop-2-yn-1-ylcarbamoyl)-*L*-leucinate (**16a**) and methyl (prop-2-yn-1-ylcarbamoyl)-*L*-alloisoleucinate (**16b**) were obtained as described previously.[31]

*5.1.1.1. (S)-Methyl 4-(methylthio)-2-(3-(prop-2-yn-1-yl)ureido)butanoate (**16c**)*

According to the similar procedures described by our group[31], compound **15c** was converted to **16c** as a white solid (2.07 g, yield 85%), mp: 70.6-72.2 °C. ^{1}H NMR (400 MHz, DMSO-d_6): δ 6.49 (d, J = 8.0 Hz, 1H), 6.30 (t, J = 8.0 Hz, 1H), 4.30-4.25 (m, 1H), 3.79 (dd, J = 8.0 Hz, J = 4.0 Hz, 2H), 3.63 (s, 3H), 3.06 (t, J = 4.0 Hz, 1H), 2.48-2.44 (m, 2H), 2.04 (s, 3H), 1.95-1.76 (m, 2H); ESI-MS m/z 245.4 $[M+H]^+$.

*5.1.2. (S)-4-Methyl-2-(3-(prop-2-yn-1-yl)ureido)pentanoic acid (**17**)*

Compound **16a** (2.26 g, 10 mmol) was added into the mixture of 1N NaOH aqueous solution (12 mL) and methanol (12 mL). After stirring at 25 ℃ for 0.5 h, 10 % HCl was added to adjust pH to 6. The aqueous layer was extracted by EtOAc and then dried over $MgSO_4$. After filtration, EtOAc was evaporated and the residue was dissolved in DCM. The mixture was placed into refrigerator for 12 h. The formed precipitate was filtered off to give 1.34 g of **17** as a white solid. Yield: 63%, mp: 76.4-78.2 °C. ^{1}H NMR (400 MHz, DMSO-d_6): δ 12.50 (s, 1H), 6.28-6.23 (m, 2H), 4.15-4.11 (m, 1H), 3.80-3.78 (m, 2H), 3.06-3.05 (m, 1H), 1.66-1.59 (m, 1H), 1.48-1.39 (m, 2H), 0.89-0.87 (m, 6H); ESI-MS m/z 213.4 $[M+H]^+$.

*5.1.3. Preparation of compounds **18a-18c***

Compounds (*S*)-*N*-hydroxy-4-methyl-2-(3-(prop-2-yn-1-yl)ureido)pentanamide (**18a**) and (2*S*,3*R*)-*N*-hydroxy-3-methyl-2-(3-(prop-2-yn-1-yl)ureido)pentanamide (**18b**) were obtained as described previously.[31]

*5.1.3.1. (S)-N-hydroxy-4-(methylthio)-2-(3-(prop-2-yn-1-yl)ureido)butanamide (**18c**)*

According to the similar procedure described by our group[31], compound **16c** was converted to **18c** as a white solid (1.35 g, yield 55%), mp: 88.6-90.2 °C. ^{1}H NMR (600 MHz, DMSO-d_6): δ 10.68 (s, 1H), 8.86 (s, 1H), 6.31-6.29 (m, 2H), 4.11-4.08 (m, 1H), 3.79-3.77 (m, 2H), 3.06-3.05 (m, 1H), 2.42-2.33 (m, 2H), 2.03 (s, 3H), 1.79-1.66 (m, 2H); ESI-MS m/z 246.4 $[M+H]^+$.

*5.1.4. Preparation of compounds **20a-20z** and **20aa***

*5.1.4.1. Azidobenzene (**20a**)*

To a solution of aniline (0.93 g, 10 mmol) in 10% HCl (50 mL) cooled in an ice-bath was added $NaNO_2$ (0.74 g, 10.7 mmol). The mixture was stirred at 0 ℃ for 0.5 h and followed by the addition of NaN_3 (0.72 g, 11 mmol). The mixture was stirred at 0 ℃ for 0.5 h and the aqueous layer was extracted by EtOAc (3 × 50 mL). The organic layer

was dried over $MgSO_4$ overnight. After filtration, EtOAc was evaporated to give **20a** as yellow oil (1.09 g, yield 92%), which was used directly in the next reaction without further purification.

Compounds **20b-20z** and **20aa** were prepared from compounds **19b-19z** and **19aa** in a similar manner as described for compound **20a**, respectively.

*5.1.5. Preparation of compounds **21**, **22a-22z**, **22aa**, **23** and **24***

*5.1.5.1. (S)-4-Methyl-2-(3-((1-phenyl-1H-1,2,3-triazol-4-yl)methyl)ureido)pentanoic acid (**21**)*

To a solution of compounds **17** (0.42 g, 2 mmol) and **20a** (0.26 g, 2.2 mmol) in DMSO (16 mL) was added sodium ascorbate (59.4 mg, 0.3 mmol) in H_2O (2 mL) and $CuSO_4{\cdot}5H_2O$ (25 mg, 0.1 mmol) in H_2O (2 mL). The mixture was stirred at 25 °C for 2 h. After addition of water (100 mL), the mixture was extracted by EtOAc (3 × 100 mL). The organic layer was washed with brine (3 × 100 mL) and dried over $MgSO_4$. EtOAc was evaporated and the residue was dissolved in DCM (30 mL). The mixture was stirred at 25 °C for 2 h. The formed precipitate was filtered off to give 0.36 g of compound **21** as a white solid. Yield: 55%, mp: 140.4-142.2 °C. ^{1}H NMR (300 MHz, DMSO-d_6): δ 12.48 (s, 1H), 8.57 (s, 1H), 7.89-7.85 (m, 2H), 7.62-7.57 (m, 2H), 7.51-7.46 (m, 1H), 6.49 (t, J = 5.7 Hz, 1H), 6.26 (d, J = 8.4 Hz, 1H), 4.35-4.32 (m, 2H), 4.17-4.09 (m, 1H), 1.71-1.58 (m, 1H), 1.48-1.40 (m, 2H), 0.90-0.85 (m, 6H); ^{13}C-NMR (75 MHz, DMSO-d_6): δ 175.2, 157.5, 146.9, 136.6, 129.8, 128.5, 120.7, 119.9, 50.9, 41.0, 34.8, 24.2, 22.7, 21.5; HRMS (AP-ESI) m/z calcd for $C_{16}H_{22}N_5O_3$ $[M+H]^+$ 332.1723, found 332.1733.

Compounds **22a-22z** and **22aa** were prepared by coupling compounds **20a-20z** and **20aa** with **18a** in a similar manner as described for compound **21**, respectively.

5.1.5.2. (S)-N-hydroxy-4-methyl-2-(3-((1-phenyl-1H-1,2,3-triazol-4-yl)methyl)ureido)

*pentanamide (**22a**)*

White solid, yield: 47%, mp: 174.2-176.2 °C. ^{1}H NMR (300 MHz, DMSO-d_6): δ 10.69 (s, 1H), 8.81 (s, 1H), 8.58 (s, 1H), 7.90-7.87 (m, 2H), 7.62-7.57 (m, 2H), 7.51-7.46 (m, 1H), 6.48 (t, J = 5.7 Hz, 1H), 6.18 (d, J = 8.7 Hz, 1H), 4.34-4.31 (m, 2H), 4.08 (q, J = 8.7 Hz, 1H), 1.66-1.43 (m, 1H), 1.37-1.32 (m, 2H), 0.88-0.84 (m, 6H); ^{13}C-NMR (75 MHz, DMSO-d_6): δ 169.4, 157.2, 146.9, 136.6, 129.8, 128.5, 120.6, 119.9, 49.1, 42.3, 34.8, 24.1, 22.7, 22.1; HRMS (AP-ESI) m/z calcd for $C_{16}H_{23}N_6O_3$ $[M+H]^+$ 347.1832, found 347.1826.

*5.1.5.3. (S)-2-(3-((1-(2-Chlorophenyl)-1H-1,2,3-triazol-4-yl)methyl)ureido)-N-hydroxyl-4-methylpentanamide (**22b**)*

White solid, yield: 61%, mp: 144.2-146.0 °C. ^{1}H NMR (600 MHz, DMSO-d_6): δ 10.68 (s, 1H), 8.80 (s, 1H), 8.31 (s, 1H), 7.77 (dd, J = 7.8 Hz, J = 1.2 Hz, 1H), 7.66 (dd, J = 7.8 Hz, J = 1.2 Hz, 1H), 7.63 (td, J = 7.8 Hz, J = 1.2 Hz, 1H),7.58 (td, J = 7.8 Hz, J = 1.2 Hz, 1H), 6.49 (t, J = 5.4 Hz, 1H), 6.20 (d, J = 9.0 Hz, 1H), 4.36-4.34 (m, 2H), 4.09 (q, J = 9.0 Hz, 1H), 1.56-1.51 (m, 1H), 1.35-1.33 (m, 2H), 0.88-0.84 (m, 6H); ^{13}C-NMR (75 MHz, DMSO-d_6): δ 169.3, 157.1, 145.9, 134.5, 131.4, 130.5, 128.4, 128.3, 128.2, 124.5, 49.0, 42.3, 34.7, 24.1, 22.7, 22.1; HRMS (AP-ESI) m/z calcd for $C_{16}H_{22}ClN_6O_3$ $[M+H]^+$ 381.1442, found 381.1435.

*5.1.5.4. (S)-2-(3-((1-(3-Chlorophenyl)-1H-1,2,3-triazol-4-yl)methyl)ureido)-N-hydroxy-4-methylpentanamide (**22c**)*

White solid, yield: 58%, mp: 176.4-178.4 °C. ^{1}H NMR (600 MHz, DMSO-d_6): δ 10.68 (s, 1H), 8.80 (s, 1H), 8.68 (s, 1H), 8.03 (s, 1H), 7.91 (d, J = 8.4 Hz, 1H), 7.62 (t, J = 8.4 Hz, 1H),7.56 (d, J = 8.4 Hz, 1H), 6.48 (t, J = 5.4 Hz, 1H), 6.18 (d, J = 9.0 Hz, 1H), 4.34-4.31 (m, 2H), 4.07 (q, J = 9.0 Hz, 1H), 1.55-1.51 (m, 1H), 1.36-1.33 (m, 2H), 0.88-0.84 (m, 6H); ^{13}C-NMR (75 MHz, DMSO-d_6): δ 169.4, 157.2, 147.1, 137.6, 134.1,

131.6, 128.3, 120.9, 119.6, 118.4, 49.1, 42.3, 34.8, 24.1, 22.7, 22.1; HRMS (AP-ESI) m/z calcd for $C_{16}H_{22}ClN_6O_3$ $[M+H]^+$ 381.1442, found 381.1453.

*5.1.5.5. (S)-2-(3-((1-(4-Chlorophenyl)-1H-1,2,3-triazol-4-yl)methyl)ureido)-N-hydroxy-4-methylpentanamide (**22d**)*

White solid, yield: 62%, mp: 180.2-182.2 °C. ^{1}H NMR (600 MHz, DMSO-d_6): δ 10.69 (s, 1H), 8.81 (s, 1H), 8.62 (s, 1H), 7.94 (d, J = 8.4 Hz, 2H), 7.67 (d, J = 8.4 Hz, 2H), 6.48 (t, J = 5.4 Hz, 1H), 6.19 (d, J = 9.0 Hz, 1H), 4.34-4.31 (m, 2H), 4.07 (q, J = 9.0 Hz, 1H), 1.55-1.51 (m, 1H), 1.35-1.33 (m, 2H), 0.88-0.84 (m, 6H); ^{13}C-NMR (75 MHz, DMSO-d_6): δ 169.3, 157.2, 147.1, 135.4, 132.7, 129.8, 121.5, 120.8, 49.1, 42.3, 34.8, 24.1, 22.7, 22.1; HRMS (AP-ESI) m/z calcd for $C_{16}H_{22}ClN_6O_3$ $[M+H]^+$ 381.1442, found 381.1445.

*5.1.5.6. (S)-2-(3-((1-(2-Bromophenyl)-1H-1,2,3-triazol-4-yl)methyl)ureido)-N-hydroxy-4-methylpentanamide (**22e**)*

White solid, yield: 66%, mp: 164.4-166.4 °C. ^{1}H NMR (600 MHz, DMSO-d_6): δ 10.68 (s, 1H), 8.79 (s, 1H), 8.28 (s, 1H), 7.92-7.91 (m, 1H), 7.62-7.54 (m, 3H), 6.48 (t, J = 5.4 Hz, 1H), 6.20 (d, J = 9.0 Hz, 1H), 4.36-4.33 (m, 2H), 4.08 (q, J = 9.0 Hz, 1H), 1.56-1.51 (m, 1H), 1.35-1.33 (m, 2H), 0.88-0.84 (m, 6H); ^{13}C-NMR (75 MHz, DMSO-d_6): δ 169.3, 157.1, 145.8, 136.2, 133.6, 131.8, 128.9, 128.5, 124.5, 118.6, 49.1, 42.3, 34.7, 24.1, 22.7, 22.1; HRMS (AP-ESI) m/z calcd for $C_{16}H_{22}BrN_6O_3$ $[M+H]^+$ 425.0937, found 425.0927.

*5.1.5.7. (S)-2-(3-((1-(3-Bromophenyl)-1H-1,2,3-triazol-4-yl)methyl)ureido)-N-hydroxy-4-methylpentanamide (**22f**)*

White solid, yield: 59%, mp: 176.4-178.2 °C. ^{1}H NMR (600 MHz, DMSO-d_6): δ 10.68 (s, 1H), 8.80 (s, 1H), 8.68 (s, 1H), 8.15 (s, 1H), 7.95 (d, J = 7.8 Hz, 1H), 7.69 (d, J = 7.8 Hz, 1H), 7.55 (t, J = 7.8 Hz, 1H), 6.48 (t, J = 5.4 Hz, 1H), 6.18 (d, J = 9.0 Hz,

1H), 4.34-4.31 (m, 2H), 4.07 (q, *J* = 9.0 Hz, 1H), 1.55-1.51 (m, 1H), 1.36-1.33 (m, 2H), 0.88-0.85 (m, 6H); ^{13}C-NMR (75 MHz, DMSO-d_6): δ 169.3, 157.1, 147.1, 137.7, 131.8, 131.2, 122.4, 120.9, 118.8, 49.1, 42.3, 34.8, 24.1, 22.7, 22.1; HRMS (AP-ESI) m/z calcd for $C_{16}H_{22}BrN_6O_3$ $[M+H]^+$ 425.0937, found 425.0944.

*5.1.5.8. (S)-2-(3-((1-(4-Bromophenyl)-1H-1,2,3-triazol-4-yl)methyl)ureido)-N-hydroxy-4-methylpentanamide (**22g**)*

White solid, yield: 64%, mp: 188.2-190.0 °C. ^{1}H NMR (600 MHz, DMSO-d_6): δ 10.68 (s, 1H), 8.80 (s, 1H), 8.62 (s, 1H), 7.87 (d, *J* = 8.4 Hz, 2H), 7.80 (d, *J* = 8.4 Hz, 2H), 6.48 (t, *J* = 5.4 Hz, 1H), 6.18 (d, *J* = 9.0 Hz, 1H), 4.34-4.30 (m, 2H), 4.07 (q, *J* = 9.0 Hz, 1H), 1.54-1.51 (m, 1H), 1.35-1.33 (m, 2H), 0.88-0.84 (m, 6H); ^{13}C-NMR (75 MHz, DMSO-d_6): δ 169.3, 157.1, 147.1, 135.8, 132.7, 121.8, 121.1, 120.7, 49.1, 42.3, 34.8, 24.1, 22.7, 22.1; HRMS (AP-ESI) m/z calcd for $C_{16}H_{22}BrN_6O_3$ $[M+H]^+$ 425.0937, found 425.0928.

*5.1.5.9. (S)-N-hydroxy-4-methyl-2-(3-((1-(o-tolyl)-1H-1,2,3-triazol-4-yl)methyl)ureido) pentanamide (**22h**)*

White solid, yield: 63%, mp: 130.4-132.4 °C. ^{1}H NMR (600 MHz, DMSO-d_6): δ 10.67 (s, 1H), 8.79 (s, 1H), 8.22 (s, 1H), 7.48-7.47 (m, 2H), 7.41-7.40 (m, 2H), 6.46 (t, *J* = 5.4 Hz, 1H), 6.17 (d, *J* = 9.0 Hz, 1H), 4.34-4.32 (m, 2H), 4.08 (q, *J* = 9.0 Hz, 1H), 2.14 (s, 3H), 1.54-1.52 (m, 1H), 1.35-1.33 (m, 2H), 0.88-0.84 (m, 6H); ^{13}C-NMR (75 MHz, DMSO-d_6): δ 169.3, 157.1, 145.7, 136.3, 132.9, 131.3, 129.6, 126.9, 125.8, 124.0, 49.1, 42.3, 34.8, 24.1, 22.7, 22.0, 17.3; HRMS (AP-ESI) m/z calcd for $C_{17}H_{25}N_6O_3$ $[M+H]^+$ 361.1988, found 361.1985.

*5.1.5.10. (S)-N-hydroxy-4-methyl-2-(3-((1-(m-tolyl)-1H-1,2,3-triazol-4-yl)methyl) ureido)pentanamide (**22i**)*

White solid, yield: 58%, mp: 174.2-176.0 °C. ^{1}H NMR (600 MHz, DMSO-d_6): δ

10.67 (s, 1H), 8.79 (s, 1H), 8.22 (s, 1H), 7.48-7.47 (m, 2H), 7.41-7.40 (m, 2H), 6.46 (t, *J* = 5.4 Hz, 1H), 6.17 (d, *J* = 9.0 Hz, 1H), 4.34-4.32 (m, 2H), 4.08 (q, *J* = 9.0 Hz, 1H), 2.14 (s, 3H), 1.54-1.52 (m, 1H), 1.35-1.33 (m, 2H), 0.88-0.84 (m, 6H); ^{13}C-NMR (75 MHz, DMSO-d_6): δ 169.3, 157.1, 145.7, 136.3, 132.9, 131.3, 129.6, 126.9, 125.8, 124.0, 49.1, 42.3, 34.8, 24.1, 22.7, 22.0, 17.3; HRMS (AP-ESI) m/z calcd for $C_{17}H_{25}N_6O_3$ $[M+H]^+$ 361.1988, found 361.1985.

*5.1.5.11. (S)-N-hydroxy-4-methyl-2-(3-((1-(p-tolyl)-1H-1,2,3-triazol-4-yl)methyl) ureido)pentanamide (**22j**)*

White solid, yield: 66%, mp: 166.4-168.2 °C. ^{1}H NMR (600 MHz, DMSO-d_6): δ 10.67 (s, 1H), 8.79 (s, 1H), 8.51 (s, 1H), 7.75 (d, *J* = 8.4 Hz, 2H), 7.39 (d, *J* = 8.4 Hz, 2H), 6.46 (t, *J* = 5.4 Hz, 1H), 6.17 (d, *J* = 9.0 Hz, 1H), 4.32-4.30 (m, 2H), 4.08 (q, *J* = 9.0 Hz, 1H), 2.38 (s, 3H), 1.54-1.52 (m, 1H), 1.35-1.33 (m, 2H), 0.88-0.84 (m, 6H); ^{13}C-NMR (75 MHz, DMSO-d_6): δ 169.4, 157.2, 146.7, 138.1, 134.4, 130.1, 120.5, 119.7, 49.1, 42.3, 34.8, 24.1, 22.7, 22.1, 20.5; HRMS (AP-ESI) m/z calcd for $C_{17}H_{25}N_6O_3$ $[M+H]^+$ 361.1988, found 361.1986.

*5.1.5.12. (S)-N-hydroxy-2-(3-((1-(2-hydroxyphenyl)-1H-1,2,3-triazol-4-yl)methyl) ureido)-4-methylpentanamide (**22k**)*

White solid, yield: 43%, mp: 80.4-82.4 °C. ^{1}H NMR (600 MHz, DMSO-d_6): δ 10.68 (s, 1H), 10.54 (s, 1H), 9.20 (s, 1H), 8.81 (s, 1H), 7.58 (d, *J* = 7.8 Hz, 1H), 7.33 (t, *J* = 7.8 Hz, 1H), 7.11 (d, *J* = 7.8 Hz, 1H), 7.00 (t, *J* = 7.8 Hz, 1H), 6.45 (t, *J* = 5.4 Hz, 1H), 6.17 (d, *J* = 8.4 Hz, 1H), 4.33-4.31 (m, 2H), 4.07 (q, *J* = 8.4 Hz, 1H), 1.55-1.50 (m, 1H), 1.35-1.33 (m, 2H), 0.88-0.84 (m, 6H); ^{13}C-NMR (75 MHz, DMSO-d_6): δ 169.3, 157.1, 149.8, 145.5, 129.8, 124.8, 124.5, 123.8, 119.1, 117.1, 49.0, 42.3, 34.8, 24.1, 22.7, 22.1; HRMS (AP-ESI) m/z calcd for $C_{16}H_{23}N_6O_3$ $[M+H]^+$ 363.1781, found 363.1784.

5.1.5.13. (S)-N-hydroxy-2-(3-((1-(3-hydroxyphenyl)-1H-1,2,3-triazol-4-yl)methyl)

*ureido)-4-methylpentanamide (**22l**)*

White solid, yield: 48%, mp: 164.4-166.4 °C. ^{1}H NMR (600 MHz, DMSO-d_6): δ 10.68 (s, 1H), 10.04 (s, 1H), 8.80 (s, 1H), 8.50 (s, 1H), 7.36 (t, J = 7.8 Hz, 1H), 7.27-7.26 (m, 2H), 6.86 (d, J = 7.8 Hz, 1H), 6.45 (t, J = 5.4 Hz, 1H), 6.17 (d, J = 8.4 Hz, 1H), 4.32-4.30 (m, 2H), 4.08 (q, J = 8.4 Hz, 1H), 1.55-1.51 (m, 1H), 1.35-1.33 (m, 2H), 0.88-0.84 (m, 6H); ^{13}C-NMR (75 MHz, DMSO-d_6): δ 169.3, 158.4, 157.1, 146.7, 137.6, 130.7, 120.6, 115.4, 110.2, 106.8, 49.1, 42.3, 34.8, 24.1, 22.7, 22.1; HRMS (AP-ESI) m/z calcd for $C_{16}H_{23}N_6O_3$ $[M+H]^+$ 363.1781, found 363.1790.

*5.1.5.14. (S)-N-hydroxy-2-(3-((1-(4-hydroxyphenyl)-1H-1,2,3-triazol-4-yl)methyl) ureido)-4-methylpentanamide (**22m**)*

White solid, yield: 49%, mp: 136.4-138.4 °C. ^{1}H NMR (600 MHz, DMSO-d_6): δ 10.68 (s, 1H), 9.92 (s, 1H), 8.80 (s, 1H), 8.38 (s, 1H), 7.63 (t, J = 8.4 Hz, 1H), 6.92 (t, J = 8.4 Hz, 2H), 6.86 (d, J = 7.8 Hz, 1H), 6.44 (t, J = 5.4 Hz, 1H), 6.16 (d, J = 9.0 Hz, 1H), 4.31-4.28 (m, 2H), 4.07 (q, J = 9.0 Hz, 1H), 1.55-1.51 (m, 1H), 1.35-1.33 (m, 2H), 0.88-0.84 (m, 6H); ^{13}C-NMR (75 MHz, DMSO-d_6): δ 169.4, 157.6, 157.2, 146.4, 128.8, 121.7, 120.5, 115.9, 49.1, 42.3, 34.8, 24.1, 22.7, 22.1; HRMS (AP-ESI) m/z calcd for $C_{16}H_{23}N_6O_3$ $[M+H]^+$ 363.1781, found 363.1779.

*5.1.5.15. (S)-N-hydroxy-2-(3-((1-(2-methoxyphenyl)-1H-1,2,3-triazol-4-yl)methyl) ureido)-4-methylpentanamide (**22n**)*

White solid, yield: 64%, mp: 130.2-132.2 °C. ^{1}H NMR (600 MHz, DMSO-d_6): δ 10.68 (s, 1H), 8.79 (s, 1H), 8.20 (s, 1H), 7.60 (d, J = 7.8 Hz, 1H), 7.52 (t, J = 7.8 Hz, 1H), 7.32 (d, J = 7.8 Hz, 1H), 7.14 (t, J = 7.8 Hz, 1H), 6.46 (t, J = 5.4 Hz, 1H), 6.19 (d, J = 9.0 Hz, 1H), 4.33-4.31 (m, 2H), 4.08 (q, J = 9.0 Hz, 1H), 3.85 (s, 3H), 1.56-1.51 (m, 1H), 1.35-1.33 (m, 2H), 0.88-0.84 (m, 6H); ^{13}C-NMR (75 MHz, DMSO-d_6): δ 169.3, 157.1, 151.4, 145.6, 130.5, 125.7, 125.5, 124.2, 120.8, 112.9, 56.0, 49.0, 42.3, 34.8,

24.1, 22.7, 22.0; HRMS (AP-ESI) m/z calcd for $C_{17}H_{25}N_6O_4$ $[M+H]^+$ 377.1937, found 377.1928.

*5.1.5.16. (S)-N-hydroxy-2-(3-((1-(3-methoxyphenyl)-1H-1,2,3-triazol-4-yl)methyl) ureido)-4-methylpentanamide (**22o**)*

White solid, yield: 68%, mp: 156.2-158.2 °C. ^{1}H NMR (600 MHz, DMSO-d_6): δ 10.67 (s, 1H), 8.79 (s, 1H), 8.61 (s, 1H), 7.50-7.45 (m, 3H), 7.05-7.04 (m, 1H), 6.47 (t, J = 5.4 Hz, 1H), 6.18 (d, J = 9.0 Hz, 1H), 4.33-4.31 (m, 2H), 4.07 (q, J = 9.0 Hz, 1H), 3.86 (s, 3H), 1.55-1.53 (m, 1H), 1.36-1.33 (m, 2H), 0.88-0.85 (m, 6H); ^{13}C-NMR (75 MHz, DMSO-d_6): δ 169.4, 160.1, 157.2, 146.8, 137.6, 130.7, 120.8, 114.3, 111.8, 105.4, 55.5, 49.1, 42.3, 34.8, 24.1, 22.7, 22.1; HRMS (AP-ESI) m/z calcd for $C_{17}H_{25}N_6O_4$ $[M+H]^+$ 377.1937, found 377.1935.

*5.1.5.17. (S)-N-hydroxy-2-(3-((1-(4-methoxyphenyl)-1H-1,2,3-triazol-4-yl)methyl) ureido)-4-methylpentanamide (**22p**)*

White solid, yield: 64%, mp: 178.2-180.0 °C. ^{1}H NMR (600 MHz, DMSO-d_6): δ 10.68 (s, 1H), 8.80 (s, 1H), 8.47 (s, 1H), 7.78 (d, J = 8.4 Hz, 2H), 7.13 (d, J = 8.4 Hz, 2H), 6.45 (t, J = 5.4 Hz, 1H), 6.17 (d, J = 9.0 Hz, 1H), 4.32-4.29 (m, 2H), 4.07 (q, J = 9.0 Hz, 1H), 3.83 (s, 3H), 1.55-1.51 (m, 1H), 1.35-1.33 (m, 2H), 0.88-0.84 (m, 6H); ^{13}C-NMR (75 MHz, DMSO-d_6): δ 169.4, 159.1, 157.1, 146.6, 130.0, 121.5, 120.6, 114.8, 55.5, 49.1, 42.3, 34.8, 24.1, 22.7, 22.1; HRMS (AP-ESI) m/z calcd for $C_{17}H_{25}N_6O_4$ $[M+H]^+$ 377.1937, found 377.1928.

*5.1.5.18. (S)-Methyl-2-(4-((3-(1-(hydroxyamino)-4-methyl-1-oxopentan-2-yl) ureido)methyl)-1H-1,2,3-triazol-1-yl)benzoate (**22q**)*

White solid, yield: 66%, mp: 144.4-146.2 °C. ^{1}H NMR (600 MHz, DMSO-d_6): δ 10.68 (s, 1H), 8.80 (s, 1H), 8.30 (s, 1H), 7.91 (d, J = 7.8 Hz, 1H), 7.80 (t, J = 7.8 Hz, 1H), 7.69 (t, J = 7.8 Hz, 1H), 7.65 (d, J = 7.8 Hz, 1H), 6.46 (t, J = 5.4 Hz, 1H), 6.21 (d,

J = 9.0 Hz, 1H), 4.34-4.31 (m, 2H), 4.08 (q, *J* = 9.0 Hz, 1H), 3.62 (s, 3H), 1.55-1.51 (m, 1H), 1.35-1.33 (m, 2H), 0.88-0.85 (m, 6H); ^{13}C-NMR (75 MHz, DMSO-d_6): δ 169.3, 165.7, 157.1, 146.0, 135.2, 132.8, 130.3, 129.8, 127.1, 125.9, 123.6, 52.3, 49.0, 42.3, 34.7, 24.1, 22.7, 22.1; HRMS (AP-ESI) m/z calcd for $C_{18}H_{25}N_6O_5$ $[M+H]^+$ 405.1886, found 405.1889.

*5.1.5.19. (S)-2-(3-((1-(2-Ethoxyphenyl)-1H-1,2,3-triazol-4-yl)methyl)ureido)-N-hydroxy-4-methylpentanamide (**22r**)*

White solid, yield: 70%, mp: 176.4-178.2 °C. ^{1}H NMR (300 MHz, DMSO-d_6): δ 10.68 (s, 1H), 8.79 (s, 1H), 8.22 (s, 1H), 7.63 (d, *J* = 7.8 Hz, 1H), 7.49 (t, *J* = 7.8 Hz, 1H), 7.30 (d, *J* = 7.8 Hz, 1H), 7.12 (t, *J* = 7.8 Hz, 1H), 6.46 (t, *J* = 5.4 Hz, 1H), 6.18 (d, *J* = 8.7 Hz, 1H), 4.33-4.31 (m, 2H), 4.19-4.05 (m, 3H), 1.60-1.47 (m, 1H), 1.37-1.28 (m, 5H), 0.88-0.84 (m, 6H); ^{13}C-NMR (75 MHz, DMSO-d_6): δ 169.3, 157.1, 150.3, 145.6, 130.3, 125.8, 125.2, 124.1, 120.8, 113.9, 64.3, 49.0, 42.4, 34.8, 24.1, 22.7, 22.1, 14.3; HRMS (AP-ESI) m/z calcd for $C_{18}H_{27}N_6O_4$ $[M+H]^+$ 391.2094, found 391.2089.

*5.1.5.20. (S)-2-(3-((1-(2,6-Dimethylphenyl)-1H-1,2,3-triazol-4-yl)methyl)ureido)-N-hydroxy-4-methylpentanamide (**22s**)*

White solid, yield: 58%, mp: 174.4-176.2 °C. ^{1}H NMR (600 MHz, DMSO-d_6): δ 10.67 (s, 1H), 8.79 (s, 1H), 8.11 (s, 1H), 7.39 (t, *J* = 7.8 Hz, 1H), 7.28 (d, *J* = 7.8 Hz, 2H), 6.44 (t, *J* = 4.8 Hz, 1H), 6.17 (d, *J* = 9.0 Hz, 1H), 4.34-4.31 (m, 2H), 4.08 (q, *J* = 9.0 Hz, 1H), 1.91 (s, 6H), 1.55-1.51 (m, 1H), 1.35-1.32 (m, 2H), 0.87-0.84 (m, 6H); ^{13}C-NMR (75 MHz, DMSO-d_6): δ 169.3, 157.1, 145.6, 135.8, 134.7, 129.8, 128.3, 124.2, 49.0, 42.4, 34.9, 24.1, 22.7, 22.0, 16.8; HRMS (AP-ESI) m/z calcd for $C_{18}H_{27}N_6O_3$ $[M+H]^+$ 375.2145, found 375.2152.

*5.1.5.21. (S)-2-(3-((1-(2,6-Dichlorophenyl)-1H-1,2,3-triazol-4-yl)methyl)ureido -N-hydroxy-4-methylpentanamide (**22t**)*

White solid, yield: 64%, mp: 170.2-172.2 °C. ^{1}H NMR (600 MHz, DMSO-d_6): δ 10.68 (s, 1H), 8.80 (s, 1H), 8.29 (s, 1H), 7.78 (d, J = 8.4 Hz, 2H), 7.68 (t, J = 8.4 Hz, 1H), 6.49 (t, J = 5.4 Hz, 1H), 6.20 (d, J = 8.4 Hz, 1H), 4.40-4.37 (m, 2H), 4.09 (q, J = 8.4 Hz, 1H), 1.55-1.51 (m, 1H), 1.35-1.33 (m, 2H), 0.88-0.84 (m, 6H); ^{13}C-NMR (75 MHz, DMSO-d_6): δ 169.3, 157.1, 145.9, 132.7, 132.7, 132.5, 129.1, 124.9, 49.0, 42.4, 34.7, 24.1, 22.7, 22.1; HRMS (AP-ESI) m/z calcd for $C_{16}H_{21}Cl_2N_6O_3$ $[M+H]^+$ 415.1052, found 415.1048.

*5.1.5.22. (S)-2-(3-((1-(2,5-Dichlorophenyl)-1H-1,2,3-triazol-4-yl)methyl)ureido)-N-hydroxy-4-methylpentanamide (**22u**)*

White solid, yield: 52%, mp: 164.4-166.4 °C. ^{1}H NMR (600 MHz, DMSO-d_6): δ 10.68 (s, 1H), 8.80 (s, 1H), 8.34 (s, 1H), 7.88 (s, 1H), 7.81 (d, J = 8.4 Hz, 1H), 7.72 (d, J = 8.4 Hz, 1H), 6.49 (t, J = 5.4 Hz, 1H), 6.20 (d, J = 9.0 Hz, 1H), 4.36-4.34 (m, 2H), 4.08 (q, J = 9.0 Hz, 1H), 1.55-1.51 (m, 1H), 1.35-1.33 (m, 2H), 0.88-0.84 (m, 6H); ^{13}C-NMR (75 MHz, DMSO-d_6): δ 169.3, 157.1, 146.0, 135.4, 132.4, 131.9, 131.2, 128.0, 127.3, 124.5, 49.0, 42.3, 34.7, 24.1, 22.7, 22.1; HRMS (AP-ESI) m/z calcd for $C_{16}H_{21}Cl_2N_6O_3$ $[M+H]^+$ 415.1052, found 415.1059.

*5.1.5.23. (S)-2-(3-((1-(2,6-Dimethoxyphenyl)-1H-1,2,3-triazol-4-yl)methyl)ureido)-N-hydroxy-4-methylpentanamide (**22v**)*

White solid, yield: 63%, mp: 168.4-170.0 °C. ^{1}H NMR (300 MHz, DMSO-d_6): δ 10.67 (s, 1H), 8.79 (s, 1H), 7.88 (s, 1H), 7.51 (t, J = 8.4 Hz, 1H), 6.87 (d, J = 8.4 Hz, 2H), 6.44 (t, J = 5.4 Hz, 1H), 6.18 (d, J = 9.0 Hz, 1H), 4.32-4.30 (m, 2H), 4.08 (q, J = 9.0 Hz, 1H), 3.72 (s, 6H), 1.61-1.48 (m, 1H), 1.37-1.32 (m, 2H), 0.88-0.84 (m, 6H); ^{13}C-NMR (75 MHz, DMSO-d_6): δ 169.4, 157.1, 155.4, 144.8, 131.5, 125.2, 114.6, 104.6, 56.0, 49.1, 42.3, 34.8, 24.1, 22.7, 22.1; HRMS (AP-ESI) m/z calcd for $C_{18}H_{27}N_6O_5$ $[M+H]^+$ 407.2043, found 407.2050.

*5.1.5.24. (S)-2-(3-((1-(2,6-Diethoxyphenyl)-1H-1,2,3-triazol-4-yl)methyl)ureido)-N-hydroxy-4-methylpentanamide (**22w**)*

White solid, yield: 63%, mp: 164.4-166.4 °C. ^{1}H NMR (300 MHz, DMSO-d_6): δ 10.68 (s, 1H), 8.79 (s, 1H), 7.85 (s, 1H), 7.45 (t, J = 8.4 Hz, 1H), 6.84 (d, J = 8.4 Hz, 2H), 6.42 (t, J = 5.4 Hz, 1H), 6.19 (d, J = 9.0 Hz, 1H), 4.32-4.30 (m, 2H), 4.13-4.00 (m, 5H), 1.61-1.47 (m, 1H), 1.36-1.32 (m, 2H), 1.16-1.11 (s, 6H), 0.88-0.84 (m, 6H); ^{13}C-NMR (75 MHz, DMSO-d_6): δ 169.3, 157.1, 154.6, 144.5, 131.3, 125.2, 115.5, 105.6, 64.3, 49.0, 42.4, 34.8, 24.1, 22.7, 22.1, 14.2; HRMS (AP-ESI) m/z calcd for $C_{20}H_{31}N_6O_5$ $[M+H]^+$ 435.2356, found 435.2344.

*5.1.5.25. (S)-2-(3-((1-(3,5-Dichlorophenyl)-1H-1,2,3-triazol-4-yl)methyl)ureido)-N-hydroxy-4-methylpentanamide (**22x**)*

White solid, yield: 65%, mp: 146.2-148.2 °C. ^{1}H NMR (600 MHz, DMSO-d_6): δ 10.68 (s, 1H), 8.80 (s, 1H), 8.75 (s, 1H), 8.06 (s, 2H), 7.76 (s, 1H), 6.50 (t, J = 5.4 Hz, 1H), 6.19 (d, J = 9.0 Hz, 1H), 4.34-4.32 (m, 2H), 4.08 (q, J = 9.0 Hz, 1H), 1.55-1.51 (m, 1H), 1.36-1.34 (m, 2H), 0.88-0.85 (m, 6H); ^{13}C-NMR (100 MHz, DMSO-d_6): δ 169.8, 157.6, 147.8, 138.7, 135.7, 128.3, 128.2, 121.5, 118.9, 118.9, 49.6, 42.8, 35.2, 24.6, 23.2, 22.6; HRMS (AP-ESI) m/z calcd for $C_{16}H_{21}Cl_2N_6O_3$ $[M+H]^+$ 415.1052, found 415.1045.

*5.1.5.26. (S)-2-(3-((1-(3,4-Dimethylphenyl)-1H-1,2,3-triazol-4-yl)methyl)ureido)-N-hydroxy-4-methylpentanamide (**22y**)*

White solid, yield: 57%, mp: 178.4-180.2 °C. ^{1}H NMR (600 MHz, DMSO-d_6): δ 10.69 (s, 1H), 8.81 (s, 1H), 8.50 (s, 1H), 7.51 (s, 2H), 7.11 (s, 1H), 6.47 (t, J = 5.4 Hz, 1H), 6.18 (d, J = 8.4 Hz, 1H), 4.33-4.30 (m, 2H), 4.08 (q, J = 8.4 Hz, 1H), 2.36 (s, 6H), 1.55-1.53 (m, 1H), 1.36-1.34 (m, 2H), 0.88-0.85 (m, 6H); ^{13}C-NMR (100 MHz, DMSO-d_6): δ 169.8, 157.7, 147.2, 138.5, 137.3, 135.0, 131.0, 121.2, 120.9, 117.6, 49.6, 42.8,

35.3, 24.6, 23.2, 22.6, 19.8, 19.4; HRMS (AP-ESI) m/z calcd for $C_{18}H_{27}N_6O_3$ $[M+H]^+$ 375.2145, found 375.2143.

*5.1.5.27. (S)-2-(3-((1-(3-Chloro-4-methylphenyl)-1H-1,2,3-triazol-4-yl)methyl) ureido)-N-hydroxy-4-methylpentanamide (**22z**)*

White solid, yield: 61%, mp: 176.2-178.0 °C. ^{1}H NMR (600 MHz, DMSO-d_6): δ 10.68 (s, 1H), 8.80 (s, 1H), 8.63 (s, 1H), 7.99 (s, 1H), 7.80 (d, J = 8.4 Hz, 1H), 7.57 (d, J = 8.4 Hz, 1H), 6.48 (t, J = 5.4 Hz, 1H), 6.18 (d, J = 8.4 Hz, 1H), 4.33-4.31 (m, 2H), 4.08 (q, J = 8.4 Hz, 1H), 2.39 (s, 3H), 1.56-1.51 (m, 1H), 1.36-1.33 (m, 2H), 0.88-0.85 (m, 6H); ^{13}C-NMR (100 MHz, DMSO-d_6): δ 169.8, 157.6, 147.5, 136.2, 136.0, 134.6, 132.7, 121.2, 120.4, 118.8, 49.6, 42.8, 35.3, 24.6, 23.2, 22.6, 19.6; HRMS (AP-ESI) m/z calcd for $C_{17}H_{24}ClN_6O_3$ $[M+H]^+$ 395.1598, found 395.1594.

*5.1.5.28. (S)-2-(3-((1-(3,5-Dimethylphenyl)-1H-1,2,3-triazol-4-yl)methyl)ureido)-N-hydroxy-4-methylpentanamide (**22aa**)*

White solid, yield: 62%, mp: 162.4-164.2 °C. ^{1}H NMR (600 MHz, DMSO-d_6): δ 10.68 (s, 1H), 8.80 (s, 1H), 8.50 (s, 1H), 7.51 (s, 2H), 7.11 (s, 1H), 6.46 (t, J = 5.4 Hz, 1H), 6.18 (d, J = 9.0 Hz, 1H), 4.33-4.30 (m, 2H), 4.08 (q, J = 9.0 Hz, 1H), 2.36 (s, 6H), 1.56-1.51 (m, 1H), 1.36-1.33 (m, 2H), 0.88-0.85 (m, 6H); ^{13}C-NMR (100 MHz, DMSO-d_6): δ 169.9, 157.7, 147.2, 139.8, 137.0, 130.2, 121.0, 117.9, 49.6, 42.8, 35.3, 24.6, 23.2, 22.6, 21.3; HRMS (AP-ESI) m/z calcd for $C_{18}H_{27}N_6O_3$ $[M+H]^+$ 375.2145, found 375.2143.

Compounds **23** and **24** were prepared by coupling compounds **18b** and **18c** with **20a** in a similar manner as described for compound **21**, respectively.

*5.1.5.29. (2S,3R)-N-hydroxy-3-methyl-2-(3-((1-phenyl-1H-1,2,3-triazol-4-yl)methyl) ureido)pentanamide (**23**)*

White solid, yield: 62%, mp: 154.4-156.0 °C. ^{1}H NMR (300 MHz, DMSO-d_6): δ

10.61 (s, 1H), 8.82 (s, 1H), 8.58 (s, 1H), 7.88 (d, *J* = 7.5 Hz, 2H), 7.60 (t, *J* = 7.5 Hz, 2H), 7.48 (t, *J* = 7.5 Hz, 1H), 6.60-6.52 (m, 1H), 6.23-6.15 (m, 2H), 4.35-4.31 (m, 2H), 4.06-3.86 (m, 1H), 1.65-1.25 (m, 2H), 1.15-0.95 (m, 1H), 0.87-0.73 (m, 6H); ^{13}C-NMR (75 MHz, DMSO-d_6): δ 157.5, 157.3, 146.8, 136.6, 129.8, 128.5, 120.6, 119.9, 54.8, 54.1, 34.8, 25.6, 15.2, 11.4; HRMS (AP-ESI) m/z calcd for $C_{16}H_{23}N_6O_3$ $[M+H]^+$ 347.1832, found 347.1824.

*5.1.5.30. (S)-N-hydroxy-4-(methylthio)-2-(3-((1-phenyl-1H-1,2,3-triazol-4-yl)methyl) ureido)butanamide (**24**)*

White solid, yield: 64%, mp: 168.4-170.2 °C. ^{1}H NMR (300 MHz, DMSO-d_6): δ 10.69 (s, 1H), 8.87 (s, 1H), 8.59 (s, 1H), 7.89 (d, *J* = 8.4 Hz, 2H), 7.60 (t, *J* = 8.4 Hz, 2H), 7.48 (t, *J* = 8.4 Hz, 1H), 6.54 (t, *J* = 5.7 Hz, 1H), 6.33 (d, *J* = 8.7 Hz, 1H), 4.35-4.33 (m, 2H), 4.13 (q, *J* = 8.7 Hz, 1H), 2.48-2.32 (m, 2H), 2.02 (s, 3H), 1.86-1.64 (m, 2H); ^{13}C-NMR (75 MHz, DMSO-d_6): δ 168.6, 157.2, 146.9, 136.6, 129.8, 128.5, 120.6, 119.9, 50.1, 34.8, 33.1, 29.3, 14.6; HRMS (AP-ESI) m/z calcd for $C_{15}H_{21}N_6O_3S$ $[M+H]^+$ 365.1396, found 365.1396.

*5.1.6. (2-nitrophenyl)methanol (**26**) and (2-aminophenyl)methanol (**27**) were obtained as described previously.*[31]

*5.1.7. (2-Azidophenyl)methanol (**28**)*

Compound **28** was prepared from compound **27** in a similar manner as described for compound **20a**. Yellow oil, yield: 93%. ^{1}H NMR (400 MHz, DMSO-d_6): δ 7.50 (d, *J* = 7.6 Hz, 1H), 7.34 (t, *J* = 7.6 Hz, 1H), 7.22-7.17 (m, 2H), 5.22 (t, *J* = 5.6 Hz, 1H), 4.48 (d, *J* = 5.4 Hz, 2H).

*5.1.8. Preparation of compounds **30a-30i***

*5.1.8.1. 2-Azidobenzyl acetate (**30a**)*

To a solution of compound **28** (1.49 g, 10 mmol) and Et_3N (1.51 g, 15 mmol) in

anhydrous THF (50 mL) was dropwise added the acetylchloride **29a** (0.94 g, 12 mmol) in anhydrous THF (10 mL) at 0 °C. The mixture was stirred at 50 °C for 3 h. After evaporation of THF, the residue was dissolved in EtOAc (3 × 100 mL). The organic layer was washed with 10% HCl (3 × 100 mL), saturated $NaHCO_3$ (3 × 100 mL) and brine (3 × 100 mL), and dried over $MgSO_4$ overnight. Evaporation of EtOAc gave compound **30a** as yellow oil (1.07 g, yield 56%). Without further purification, the crude product was used directly in the next reaction.

Compounds **30b-30i** were prepared from compounds **29b-29i** in a similar manner as described for compound **30a**, respectively.

*5.1.9. Preparation of compounds **31a-31i***

Compounds **31a-31i** were prepared by coupling compounds **30a-30i** with **18a** in a similar manner as described for compound **21**, respectively.

*5.1.9.1. (S)-2-(4-((3-(1-(Hydroxyamino)-4-methyl-1-oxopentan-2-yl)ureido)methyl)-1H-1,2,3-triazol-1-yl)benzyl acetate (**31a**)*

White solid, yield: 53%, mp: 122.2-124.0 °C. ^{1}H NMR (300 MHz, DMSO-d_6): δ 10.68 (s, 1H), 8.80 (s, 1H), 8.26 (s, 1H), 7.67-7.49 (m, 4H), 6.48 (t, J = 5.7 Hz, 1H), 6.19 (d, J = 9.0 Hz, 1H), 4.99 (s, 2H), 4.40-4.28 (m, 2H), 4.08 (q, J = 9.0 Hz, 1H), 1.96 (s, 3H), 1.60-1.32 (m, 1H), 1.24-1.17 (m, 2H), 0.88-0.84 (m, 6H); ^{13}C-NMR (75 MHz, DMSO-d_6): δ 169.8, 169.3, 157.1, 146.0, 135.5, 131.1, 129.9, 129.8, 129.3, 125.8, 124.1, 61.6, 49.1, 42.3, 34.7, 24.1, 22.7, 22.1, 20.4; HRMS (AP-ESI) m/z calcd for $C_{19}H_{27}N_6O_5$ $[M+H]^+$ 419.2043, found 419.2039.

*5.1.9.2. (S)-2-(4-((3-(1-(Hydroxyamino)-4-methyl-1-oxopentan-2-yl)ureido)methyl)-1H-1,2,3-triazol-1-yl)benzyl benzoate (**31b**)*

White solid, yield: 63%, mp: 132.4-134.2 °C. ^{1}H NMR (300 MHz, DMSO-d_6): δ 10.68 (s, 1H), 8.80 (s, 1H), 8.35 (s, 1H), 7.88-7.85 (m, 2H), 7.79-7.76 (m, 1H), 7.69-

7.49 (m, 6H), 6.48 (t, *J* = 5.7 Hz, 1H), 6.19 (d, *J* = 8.7 Hz, 1H), 5.31 (s, 2H), 4.40-4.28 (m, 2H), 4.08 (q, *J* = 9.0 Hz, 1H), 1.60-1.32 (m, 1H), 1.24-1.17 (m, 2H), 0.88-0.84 (m, 6H); ^{13}C-NMR (75 MHz, DMSO-d_6): δ 169.3, 165.1, 157.1, 146.0, 135.5, 133.4, 131.0, 129.9, 129.9, 129.4, 129.1, 129.1, 128.7, 125.8, 124.0, 62.4, 49.1, 42.3, 34.7, 24.1, 22.7, 22.1; HRMS (AP-ESI) m/z calcd for $C_{24}H_{29}N_6O_5$ $[M+H]^+$ 481.2199, found 481.2202.

*5.1.9.3. (S)-2-(4-((3-(1-(Hydroxyamino)-4-methyl-1-oxopentan-2-yl)ureido)methyl)-1H-1,2,3-triazol-1-yl)benzyl 2-methoxybenzoate (**31c**)*

White solid, yield: 66%, mp: 166.4-168.2 °C. ^{1}H NMR (300 MHz, DMSO-d_6): δ 10.69 (s, 1H), 8.80 (s, 1H), 8.36 (s, 1H), 7.88-7.85 (m, 2H), 7.79-7.77 (m, 1H), 7.67-7.52 (m, 5H), 7.15 (d, *J* = 8.4 Hz, 1H), 7.01 (t, *J* = 8.4 Hz, 1H), 6.50 (t, *J* = 5.4 Hz, 1H), 6.19 (d, *J* = 8.7 Hz, 1H), 5.23 (s, 2H), 4.36-4.34 (m, 2H), 4.09 (q, *J* = 8.7 Hz, 1H), 3.82 (s, 3H), 1.60-1.47 (m, 1H), 1.37-1.32 (m, 2H), 0.88-0.83 (m, 6H); ^{13}C-NMR (75 MHz, DMSO-d_6): δ 169.3, 165.0, 158.3, 157.1, 146.0, 135.4, 133.8, 130.9, 130.8, 129.8, 129.7, 129.3, 125.6, 124.0, 120.0, 119.2, 112.5, 62.0, 55.7, 49.1, 42.3, 34.7, 24.1, 22.7, 22.1; HRMS (AP-ESI) m/z calcd for $C_{25}H_{31}N_6O_6$ $[M+H]^+$ 511.2305, found 511.2296.

*5.1.9.4. (S)-2-(4-((3-(1-(Hydroxyamino)-4-methyl-1-oxopentan-2-yl)ureido)methyl)-1H-1,2,3-triazol-1-yl)benzyl 4-methoxybenzoate (**31d**)*

White solid, yield: 58%, mp: 120.4-122.2 °C. ^{1}H NMR (300 MHz, DMSO-d_6): δ 10.68 (s, 1H), 8.80 (s, 1H), 8.34 (s, 1H), 7.85-7.80 (m, 2H), 7.77-7.74 (m, 1H), 7.66-7.53 (m, 3H), 7.06-7.00 (m, 2H), 6.48 (t, *J* = 5.7 Hz, 1H), 6.20 (d, *J* = 9.0 Hz, 1H), 5.27 (s, 2H), 4.33-4.31 (m, 2H), 4.09 (q, *J* = 9.0 Hz, 1H), 3.83 (s, 3H), 1.60-1.47 (m, 1H), 1.37-1.32 (m, 2H), 0.87-0.83 (m, 6H); ^{13}C-NMR (75 MHz, DMSO-d_6): δ 169.4, 164.8, 163.3, 157.2, 146.1, 135.5, 131.3, 131.3, 129.9, 129.8, 129.4, 125.9, 124.1, 121.3, 114.0, 62.0, 55.5, 49.1, 42.4, 34.8, 24.1, 22.7, 22.1; HRMS (AP-ESI) m/z calcd for $C_{25}H_{31}N_6O_6$ $[M+H]^+$ 511.2305, found 511.2313.

*5.1.9.5. (S)-2-(4-((3-(1-(Hydroxyamino)-4-methyl-1-oxopentan-2-yl)ureido)methyl)-1H-1,2,3-triazol-1-yl)benzyl 2-phenylacetate (**31e**)*

White solid, yield: 56%, mp: 98.4-99.2 °C. ^{1}H NMR (300 MHz, DMSO-d_6): δ 10.68 (s, 1H), 8.80 (s, 1H), 8.23 (s, 1H), 7.62-7.49 (m, 4H), 7.38-7.20 (m, 5H), 6.48 (t, J = 5.7 Hz, 1H), 6.19 (d, J = 8.7 Hz, 1H), 5.04 (s, 2H), 4.35-4.31 (m, 2H), 4.09 (q, J = 8.7 Hz, 1H), 3.63 (s, 2H), 1.57-1.46 (m, 1H), 1.36-1.31 (m, 2H), 0.87-0.83 (m, 6H); ^{13}C-NMR (75 MHz, DMSO-d_6): δ 169.4, 165.6, 157.1, 146.0, 145.0, 135.5, 133.8, 131.1, 130.5, 129.8, 129.3, 128.8, 128.4, 125.8, 124.1, 117.4, 61.6, 59.7, 49.1, 42.3, 34.8, 24.1, 22.7, 22.1; HRMS (AP-ESI) m/z calcd for $C_{25}H_{31}N_6O_5$ $[M+H]^+$ 495.2356, found 495.2347.

*5.1.9.6. (S)-2-(4-((3-(1-(Hydroxyamino)-4-methyl-1-oxopentan-2-yl)ureido)methyl)-1H-1,2,3-triazol-1-yl)benzyl 1-naphthoate (**31f**)*

White solid, yield: 69%, mp: 136.4-138.2 °C. ^{1}H NMR (300 MHz, DMSO-d_6): δ 10.69 (s, 1H), 8.81 (s, 1H), 8.69 (d, J = 1.2 Hz, 1H), 8.40 (s, 1H), 8.20 (d, J = 8.4 Hz, 1H), 8.05-8.00 (m, 2H), 7.85-7.82 (m, 1H), 7.68-7.55 (m, 6H), 6.50 (t, J = 5.7 Hz, 1H), 6.20 (d, J = 8.7 Hz, 1H), 5.41 (s, 2H), 4.37-4.32 (m, 2H), 4.10 (q, J = 8.7 Hz, 1H), 1.60-1.47 (m, 1H), 1.37-1.32 (m, 2H), 0.87-0.83 (m, 6H); ^{13}C-NMR (75 MHz, DMSO-d_6): δ 169.3, 166.1, 157.1, 146.1, 135.6, 133.5, 133.3, 130.9, 130.3, 130.2, 130.0, 129.9, 129.5, 128.6, 127.9, 126.3, 126.0, 125.8, 124.9, 124.8, 124.0, 62.6, 49.1, 42.3, 34.7, 24.1, 22.7, 22.1; HRMS (AP-ESI) m/z calcd for $C_{28}H_{31}N_6O_5$ $[M+H]^+$ 531.2356, found 531.2350.

*5.1.9.7. (S)-2-(4-((3-(1-(Hydroxyamino)-4-methyl-1-oxopentan-2-yl)ureido)methyl)-1H-1,2,3-triazol-1-yl)benzyl [1,1'-biphenyl]-4-carboxylate (**31g**)*

White solid, yield: 68%, mp: 108.4-110.2 °C. ^{1}H NMR (300 MHz, DMSO-d_6): δ 10.68 (s, 1H), 8.80 (s, 1H), 8.37 (s, 1H), 7.95 (d, J = 8.4 Hz, 2H), 7.83-7.73 (m, 5H), 7.68-7.41 (m, 6H), 6.50 (t, J = 5.4 Hz, 1H), 6.20 (d, J = 9.0 Hz, 1H), 5.33 (s, 2H), 4.34-

4.32 (m, 2H), 4.13-4.07 (m, 1H), 1.57-1.46 (m, 1H), 1.36-1.31 (m, 2H), 0.88-0.82 (m, 6H); ^{13}C-NMR (75 MHz, DMSO-d_6): δ 169.4, 165.0, 157.2, 146.1, 144.8, 138.7, 135.5, 131.0, 129.9, 129.8, 129.4, 129.0, 128.4, 127.9, 126.9, 126.9, 125.8, 124.0, 62.4, 49.1, 42.3, 34.8, 24.1, 22.6, 22.1; HRMS (AP-ESI) m/z calcd for $C_{30}H_{33}N_6O_5$ $[M+H]^+$ 557.2512, found 557.2509.

*5.1.9.8. (S)-2-(4-((3-(1-(Hydroxyamino)-4-methyl-1-oxopentan-2-yl)ureido)methyl)-1H-1,2,3-triazol-1-yl)benzyl cyclohexanecarboxylate (**31h**)*

White solid, yield: 64%, mp: 138.2-140.0 °C. ^{1}H NMR (300 MHz, DMSO-d_6): δ 10.68 (s, 1H), 8.80 (s, 1H), 8.29 (s, 1H), 7.69-7.48 (m, 4H), 6.47 (t, J = 5.4 Hz, 1H), 6.19 (d, J = 9.0 Hz, 1H), 5.02 (s, 2H), 4.34-4.33 (m, 2H), 4.08 (q, J = 9.0 Hz, 1H), 2.28-2.20 (m, 2H), 1.76-1.71 (m, 2H), 1.62-1.49 (m, 4H), 1.37-1.32 (m, 2H), 1.27-1.12 (m, 5H), 0.88-0.84 (m, 6H); ^{13}C-NMR (75 MHz, DMSO-d_6): δ 174.3, 169.3, 157.1, 145.9, 135.4, 131.1, 129.8, 129.7, 129.3, 125.8, 123.9, 61.5, 49.1, 42.4, 41.8, 34.7, 28.3, 25.2, 24.6, 24.1, 22.7, 22.1; HRMS (AP-ESI) m/z calcd for $C_{24}H_{35}N_6O_5$ $[M+H]^+$ 487.2669, found 487.2678.

*5.1.9.9. (S)-2-(4-((3-(1-(Hydroxyamino)-4-methyl-1-oxopentan-2-yl)ureido)methyl)-1H-1,2,3-triazol-1-yl)benzyl cinnamate (**31i**)*

White solid, yield: 67%, mp: 124.4-126.4 °C. ^{1}H NMR (300 MHz, DMSO-d_6): δ 10.68 (s, 1H), 8.80 (s, 1H), 8.34 (s, 1H), 7.75-7.72 (m, 3H), 7.66-7.52 (m, 4H), 7.45-7.42 (m, 3H), 6.65-6.60 (m, 1H), 6.48 (t, J = 5.4 Hz, 1H), 6.19 (d, J = 8.7 Hz, 1H), 5.17 (s, 2H), 4.34-4.33 (m, 2H), 4.13-3.99 (m, 1H), 1.58-1.49 (m, 1H), 1.37-1.32 (m, 2H), 0.88-0.83 (m, 6H); ^{13}C-NMR (75 MHz, DMSO-d_6): δ 170.6, 169.3, 157.1, 146.0, 135.5, 134.0, 130.9, 129.7, 129.6, 129.4, 129.3, 128.5, 128.3, 128.2, 126.8, 125.8, 124.0, 61.9, 49.1, 42.3, 34.7, 24.1, 22.7, 22.1; HRMS (AP-ESI) m/z calcd for $C_{26}H_{31}N_6O_5$ $[M+H]^+$ 507.2356, found 507.2351.

5.2. Biological evaluation

5.2.1. APN inhibition assay

The inhibitory activities of target compounds against APN were determined by using L-Leu-*p*-nitroanilide as substrate and microsomal APN from porcine kidney microsomes (Biocol) in 50 mM PBS, pH 7.2 as enzyme. Briefly, inhibitors (40 μL), PBS (145 μL), substrate (5 μL, 16 mM/L) and APN solution (10 μL) were added into 96-well plates. The mixture was incubated at 37 °C for 30 min. The hydrolysis product *p*-nitroanilide was measured at 405 nm with a plate reader (Varioskan, Thermo, USA).

5.2.2. Enzyme inhibition assay towards APN from ES-2 or PLC/PRF/5 cell surfaces

Inhibitory activities against APN on ES-2 or PLC/PRF/5 cell surfaces were estimated by using L-Leu-*p*-nitroanilide as substrate and ES-2 cells or PLC/PRF/5 cells, pH 7.4 as enzyme. The inhibitors (20 μL), PBS buffer (100 μL), the substrate (10 μL, 16 mM/L) and ES-2 cells (70 μL, 2.8×10^6/mL) or PLC/PRF/5 cells (70 μL, 2.8×10^6/mL) suspension were added into 96-well plates. Then, the mixture was incubated at 37 °C for 1 h. After centrifugation, the hydrolysis product *p*-nitroanilide in the supernatant was monitored at 405 nm with a plate reader (Varioskan, Thermo, USA).

5.2.3. Anti-proliferation assay

Cells were grown in RPMI 1640 medium with 10% FBS at 37 °C in 5% CO_2 humidified incubator. The tests were evaluated by the MTT [(3-[4,5-dimethyl-2-thiazolyl]-2,5-diphenyl-2H-tetrazolium bromide)] method. Briefly, cells (100 μL) were plated in 96-well plates and allowed to grow for 4 h, and then treated with different concentrations of inhibitors (100 μL) for 48 h. MTT solution (20 μL/well, 5 mg/mL) was added and the mixture was incubated for additional 4 h. Then the medium were removed and DMSO (200 μL) was added. The mixture was shook for 15 min. The

optical density was then measured using an ELISA reader at 570 nm (Varioskan, Thermo, USA).

5.2.4. HUVEC tubular structure formation assay

Matrigel (50 μL; BD biosciences) was added into test well of 96-well plates and then allowed to gel for 0.5 h at 37 °C. HUVECs were suspended in M199 medium (5% FBS) at a density of 4×10^5 cells/mL. 50 μL of cell suspension and 50 μL of inhibitors at the tested concentrations were added to the wells coated with matrigel and incubated for 4 h at 37 °C in 5% CO_2. The branched structure was visualized by inverted microscope at 40× magnification. Images of five random fields per well were analyzed by Motic Image Plus 2.0 software (Motic Instruments Inc., Canada). The numbers of branched points of the tubular structures were counted and the average numbers were calculated. Experiments were repeated three times.

5.2.5. Rat aortic ring assay

The thoracic aortas separated from 8- to 10-week-old male Sprague Dawley rats were cut into 1-mm-long cross-section. Matrigel (100 μL; BD bioscience) was added into 96-wells plates and then allowed to polymerize for 0.5 h at 37 °C. The prepared rat aortic rings were placed into test well of 96-well plates and then covered with 100 μL of matrigel (BD bioscience). The mixture was incubated at 37 °C for 0.5 h followed by the addition of the tested compounds. After incubation for 9 days at 37 °C in 5% CO_2, the formed micro-vessels were photographed by inverted microscope at 100× magnification. The culture medium containing tested compounds was changed every three days. The results were evaluated by relative area covered with microvessels using Image-pro Plus 6.0.[34] Experiments were repeated three times. All experiments involving laboratory animals were performed with the approval by the institutional guidelines of Animal Care and Use Committee at Shandong University.

5.2.6. Anti-invasion assay

At the beginning of the assay, the BD BioCoat™ Matrigel™ Invasion Chambers were rehydrated with 500 μL of RPMI-1640 culture medium with 1% FBS in both of the upper and lower chambers for 2 h. After the medium was removed, RPMI-1640 culture medium with 10% FBS (750 μL) and RPMI-1640 culture medium with 1% FBS (100 μL) containing the tested inhibitors were added into the lower chambers and the upper chambers, respectively. Then, ES-2 cells in RPMI-1640 culture medium with 1% FBS (400 μL, 2.5×10^5 cells/mL) was added into the upper chambers. The mixture was incubated at 37 °C in 5% CO_2 for 8 h. After that, matrigel and cells in the upper chambers were erased with a cotton swab. The remained cells were fixed with methanol, and stained with 0.1% crystal violet. The photographs were taken under an inverted microscope. The results were evaluated by counting the number of cells in five random fields (100×) per well. The inhibition rate (%) of ES-2 cell invasion = [(the number of the ES-2 cells in the control group) – (the number of the ES-2 cells in the tested group)] / (the number of the ES-2 cells in the control group) × 100%. Experiments were repeated three times.

5.2.7. In vivo H22 tumor transplant model

All experiments involving laboratory animals were performed with the approval by the institutional guidelines of Animal Care and Use Committee at Shandong University. The mouse hepatoma H22 cell line was obtained from Professor Jia (Shandong Academy of Medical Sciences, China) as a kind gift. Six-week old male Kunming mice were purchased from Center for New Drugs Evaluation of Shandong University, China. To establish a H22 tumor transplant model, H22 cells (0.2 mL, 2.5×10^7/mL) were injected subcutaneously into the right anterior flank of mice. Seven days after H22 cell inoculation, the mice were randomly divided into treatment and control group. PBS, 20

mg/kg of 5-Fu, 82 mg/kg of **31f,** 82 mg/kg of **31f** plus 20 mg/kg of 5-Fu, 47 mg/kg of bestatin plus 20 mg/kg of 5-Fu were injected intraperitoneally for 14 consecutive days. The body weight was monitored every two days. After treatment, the mice were sacrificed and the H22 tumors in anterior flank were removed for weighting. The tumor growth inhibitory rate (TGI) was calculated as the following equation: TGI (%) = (average tumor weight of PBS group – average tumor weight of treatment group) / average tumor weight of PBS group × 100 %.

5.3. Statistical analysis

The statistical significance of differences between the groups was assessed by Student's *t* test. $P < 0.05$ was considered as statistically significant.

Declaration of interest

None

Acknowledgements

This work was supported by Natural Science Foundation of Shandong Province (Grant No. ZR2018QH007), National Natural Science Foundation of China (Grant No. 81373282), Key Research and Development Program of Shandong Province (2017CXGC1401), Major Project of Science and Technology of Shandong Province (2015ZDJS04001), Young Scholars Program of Shandong University (YSPSDU, Grant No. 2016WLJH33).

References

1. Antczak C, De Meester I, Bauvois B. *Bioessays.* 2001; 23:251-260.
2. Rawlings ND, Barrett AJ. *Nucleic Acids Res.* 1999; 27:325-331.
3. Olsen J, Cowell GM, Kønigshøfer E, et al. *FEBS Lett.* 1988; 238:307-314.
4. Hooper, NM. *FEBS Lett.* 1994; 354:1-6.
5. Mina-Osorio P. *Trends. Mol. Med.* 2008; 14:361-371.

6. Menrad A, Speicher D, Wacker J, Herlyn M. *Cancer Res.* 1993; 53:1450-1455.

7. Liu S, Xie F, Wang H, et al. *Oncol Rep*. 2015; 33:1372-1380.

8. Hashida H, Takabayashi A, Kanai M, et al. *Gastroenterology.* 2002; 122:376-386.

9. Ishii K, Usui S, Sugimura Y, Yamamoto H, Yoshikawa K, Hirano K. *Biol Pharm Bull. 2*001; 24:226-230.

10. Carl-McGrath S, Lendeckel U, Ebert M, Wolter AB, Roessner A, Röcken C. *Int J oncol*. 2004; 25:1223-1232.

11. Tokuhara T, Hattori N, Ishida H, et al. *Clin Cancer Res.* 2006; 12:3971-3978.

12. Saiki I, Murata J, Watanabe K, Fujii H, Abe F, Azuma I. *Jpn J Cancer Res.* 1989; 80:873-878.

13. Saiki I, Fujii H, Yoneda J, et al. *Int J Cancer.* 1993; 54:137-143.

14. Aozuka Y, Koizumi K, Saitoh Y, Ueda Y, Sakurai H, Saiki I. *Cancer Lett.* 2004; 216:35-42.

15. Fujii H, Nakajima M, Saiki I, Yoneda J, Azuma I, Tsuruo T. *Clin Exp Metastasis.* 1995; 13:337-344.

16. Yoneda J, Saiki I, Fujii H, Abe F, Kojima Y, Azuma I. *Clin Exp Metastasis.* 1992; 10:49-59.

17. Guzman-Rojas L, Rangel R, Salameh A, et al. *Proc. Natl. Acad. Sci. U S A*. 2012; 109:1637-1642.

18. Haraguchi N, Ishii H, Mimori K, et al. *J Clin Invest.* 2010; 120:3326-3339.

19. Bauvois B, Dauzonne D. *Med Res Rev.* 2006; 26:88-130.

20. Mucha A, Drag M, Dalton JP, Kafarski P. *Biochimie*. 2010; 92:1509-1529.

21. Amin SA, Adhikari N, Jha T. *J. Med. Chem.* 2018; 61:6468–6490.

22. Mishima Y, Terui Y, Sugimura N, et al. *Cancer Sci.* 2007; 98:364-372.

23. Mishima Y, Terui Y, Sugimura N, et al. *Pol J Vet Sci.* 2011; 14:393-403.

24. Jiang Y, Li X, Hou J, et al. *Eur J Med Chem.* 2018; 143:334-347.

25. Jiang Y, Hou J, Li X, et al. *Bioorg Med Chem.* 2016; 24:5787-5795.

26. Jiang Y, Li X, Hou J, et al. *Eur J Med Chem.* 2016; 121:649-657.

27. Su L, Jia Y, Wang X, Zhang L, Fang H, Xu W. *Bioorg Med Chem Lett.* 2013; 23:2512-2517.

28. Su L, Cao J, Jia Y, Zhang X, Fang H, Xu W. *ACS Med Chem Lett.* 2012; 3:959-964.

29. Ma C, Cao J, Liang X, et al. *Eur J Med Chem.* 2016; 108:21-27.

30. Ma C, Jin K, Cao J, Zhang L, Li X, Xu W. *Bioorg Med Chem.* 2013; 21:1621-1627.

31. Cao J, Ma C, Zang J, et al. *Bioorg Med Chem.* 2018; 26:3145-3157.

32. Yamashita M, Wada H, Eguchi H, et al. *Int J Oncol.* 2016; 49:89-98.

33. Chou, T.C. *Cancer. Res.* 2010; 70:440-446.

34. Blatt RJ, Clark AN, Courtney J, Tully C, Tucker AL. *Comput Methods Programs Biomed.* 2004; 75:75-79.

Graphical abstract

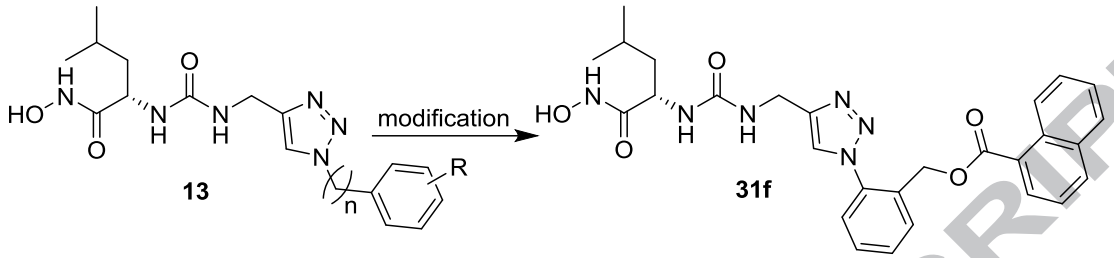

13a, n = 1, R = H, APN IC_{50} = 2.1 μM;

13b, n = 2, R = H, APN IC_{50} = 3.6 μM

31f APN IC_{50} = 0.032 μM

Highlights

> Some compounds presented sub-micromolar inhibitory activities against APN.

> The structure-activity relationship study presented that the conformational restriction was beneficial for APN inhibition.

> The best compound **31f** demonstrated promising potent *in vitro* anti-angiogenesis activity and *in vitro* anti-invasion activity.

> When combined with 5-fluorouracil (5-Fu), **31f** exhibited synergistic anti-proliferation effect against several tumor cell lines.

> Considerable *in vivo* antitumor potencies of **31f** alone or in combination with 5-Fu were observed.